

## Electronic Supporting Information (ESI)

### Mo(VI) complexes of amide-imine conjugates for tuning the selectivity of fluorescence recognition of Y(III) vs. Pb(II)

Sudeshna Chatterjee, Sabyasachi Ta, Somnath Khanra, and Debasis Das\*

Department of Chemistry, The University of Burdwan, Burdwan, 713104, W.B., India

#### 1. General method of UV-Vis and fluorescence titration

Stock solution of **M1** and **M2** are prepared (20  $\mu$ M) in HEPES buffered EtOH/H<sub>2</sub>O (4/1, v/v) media, pH 7 for UV-Vis and fluorescence titrations. Working solutions of **M1**, **M2** and Y<sup>3+</sup>, Pb<sup>2+</sup> are prepared from their respective stock solutions. The cells having path length 1 cm are used for absorption and emission studies. Fluorescence measurements have been performed using 5 nm x 5 nm slit width.

#### 2. Job's plot from fluorescence experiment

A series of solutions containing **M1**, **M2** and Y<sup>3+</sup>, Pb<sup>2+</sup> are prepared such that the total concentration of Y<sup>3+</sup>, Pb<sup>2+</sup> and **M1**, **M2** remained constant (20  $\mu$ M) in all the sets. The mole fractions ( $x$ ) of **M1** and **M2** are varied from 0.1 to 0.9. The fluorescence intensity at 527 nm and 503 nm for **M1-Y<sup>3+</sup>** and **M1-Pb<sup>2+</sup>** are plotted respectively against the mole fraction of Y<sup>3+</sup> and Pb<sup>2+</sup>. Similarly the fluorescence intensity at 497 nm for **M2-Y<sup>3+</sup>** is plotted against the mole fraction of Y<sup>3+</sup>.

#### 3. Determination of binding constant

The binding constants of **M1** and **M2** for sensed cations are determined using Benesi-Hildebrand equation:

$$\frac{F_{\max} - F_{\min}}{F_x - F_{\min}} = 1 + \frac{1}{K[C]^n}$$

Here  $F_{\min}$ ,  $F_x$ , and  $F_{\max}$  are the emission intensities of **M1** and **M2** in absence of cation, at an intermediate cation concentration, and at a concentration of complete interaction with cation respectively.  $K$  is the binding constant,  $C$  is the concentration of cation and  $n$  is the number of cation bound per molecule (here,  $n = 1$ ). The value of  $K$  can be determined from the slopes of the plots.

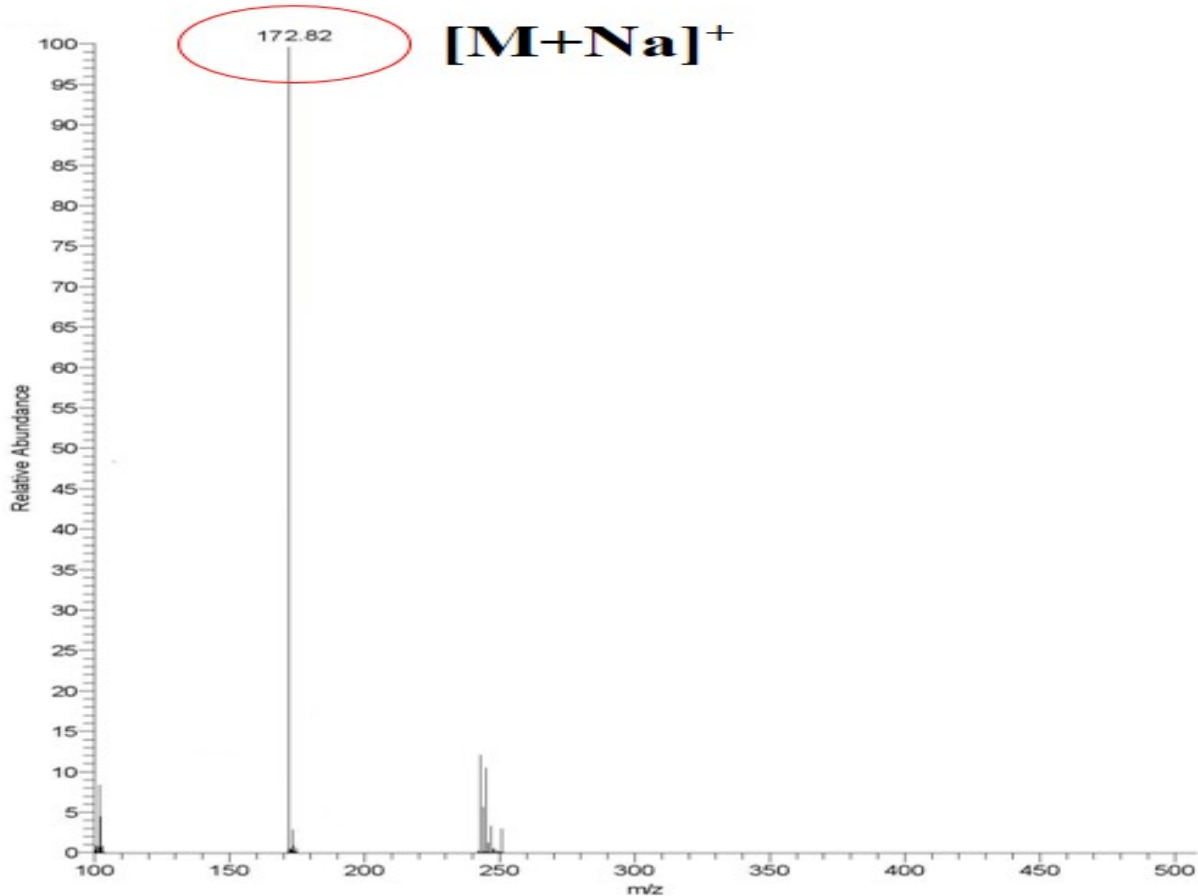
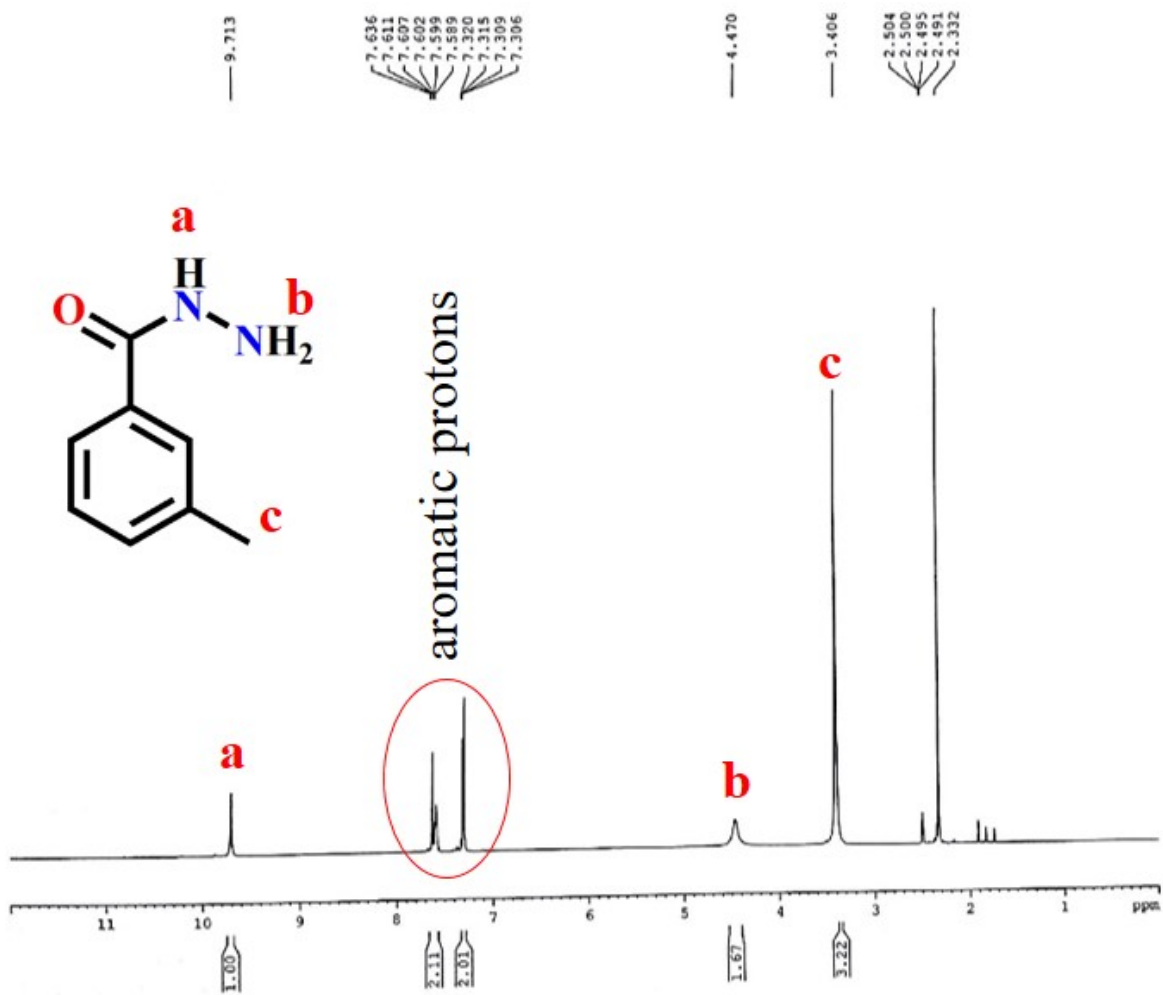
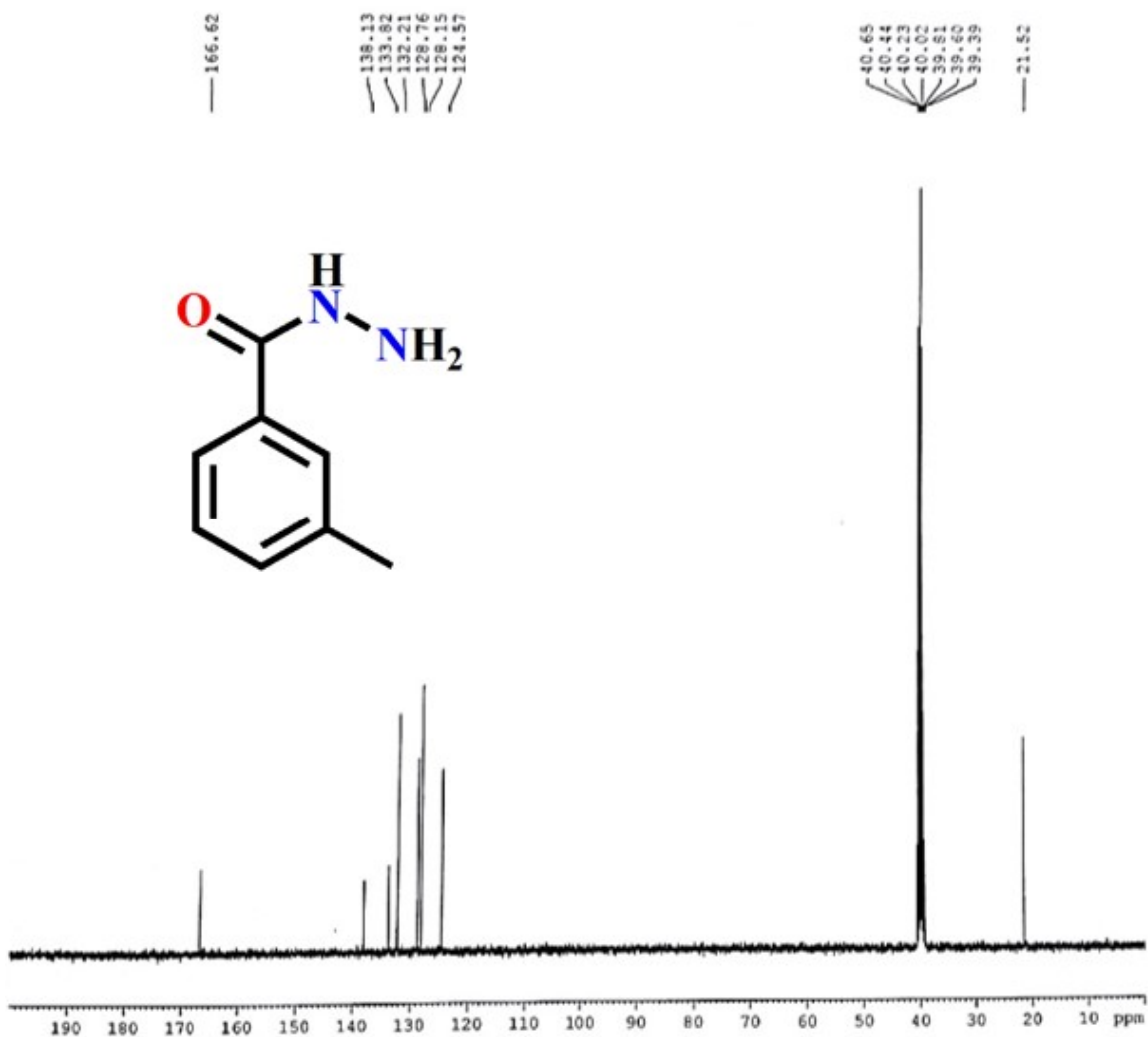


Figure S1aQTOF mass spectrum of MTA



**Figure S1b** <sup>1</sup>H NMR spectrum of MTA in DMSO-*d*<sub>6</sub>



**Figure S1c**  $^{13}\text{C}$  NMR spectrum of MTA

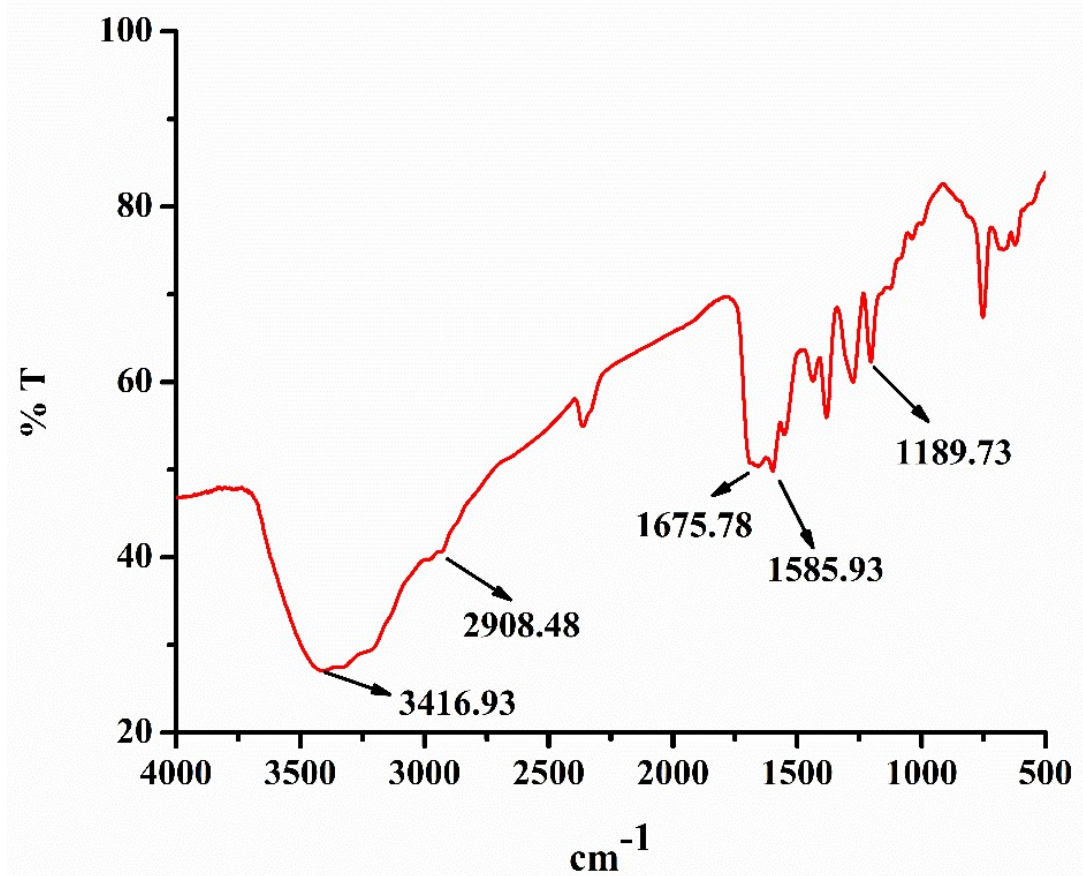


**Figure S1d** FTIR spectrum of MTA

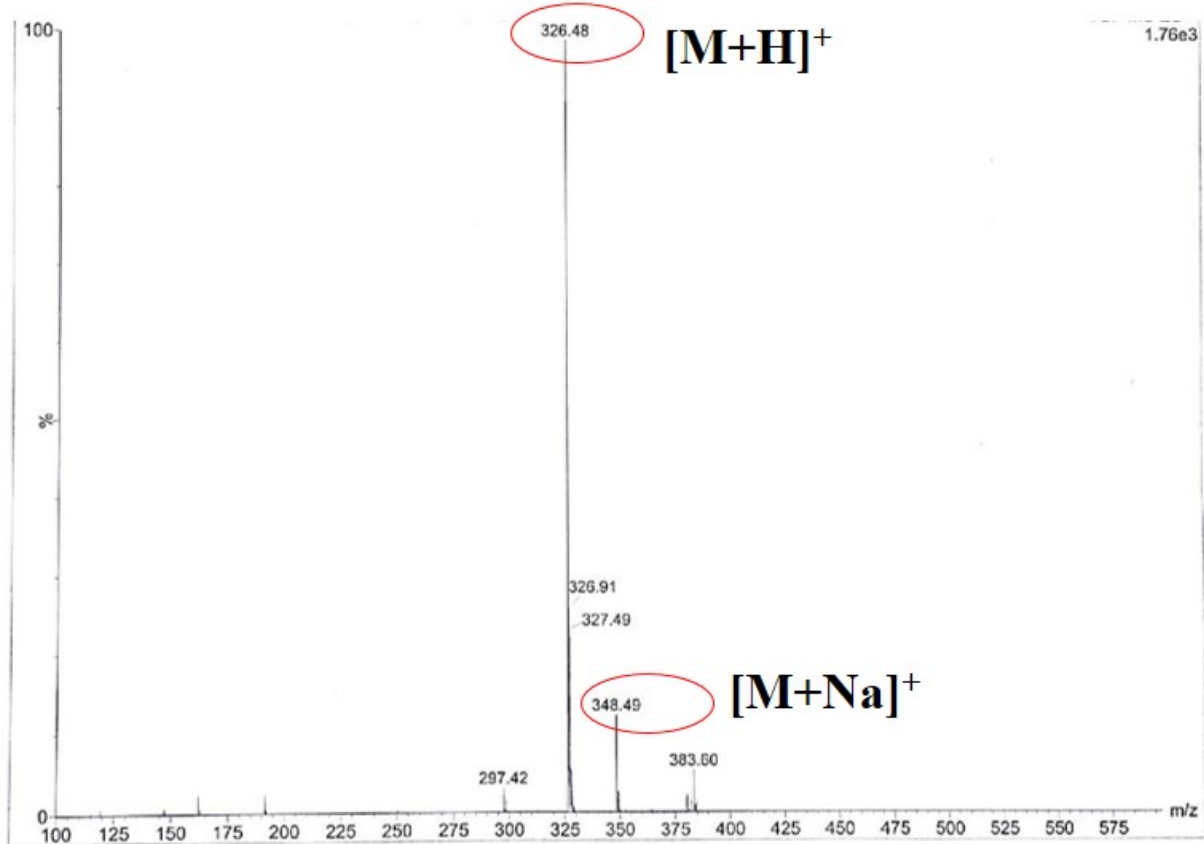


Figure S2aQTOF mass spectrum of L1

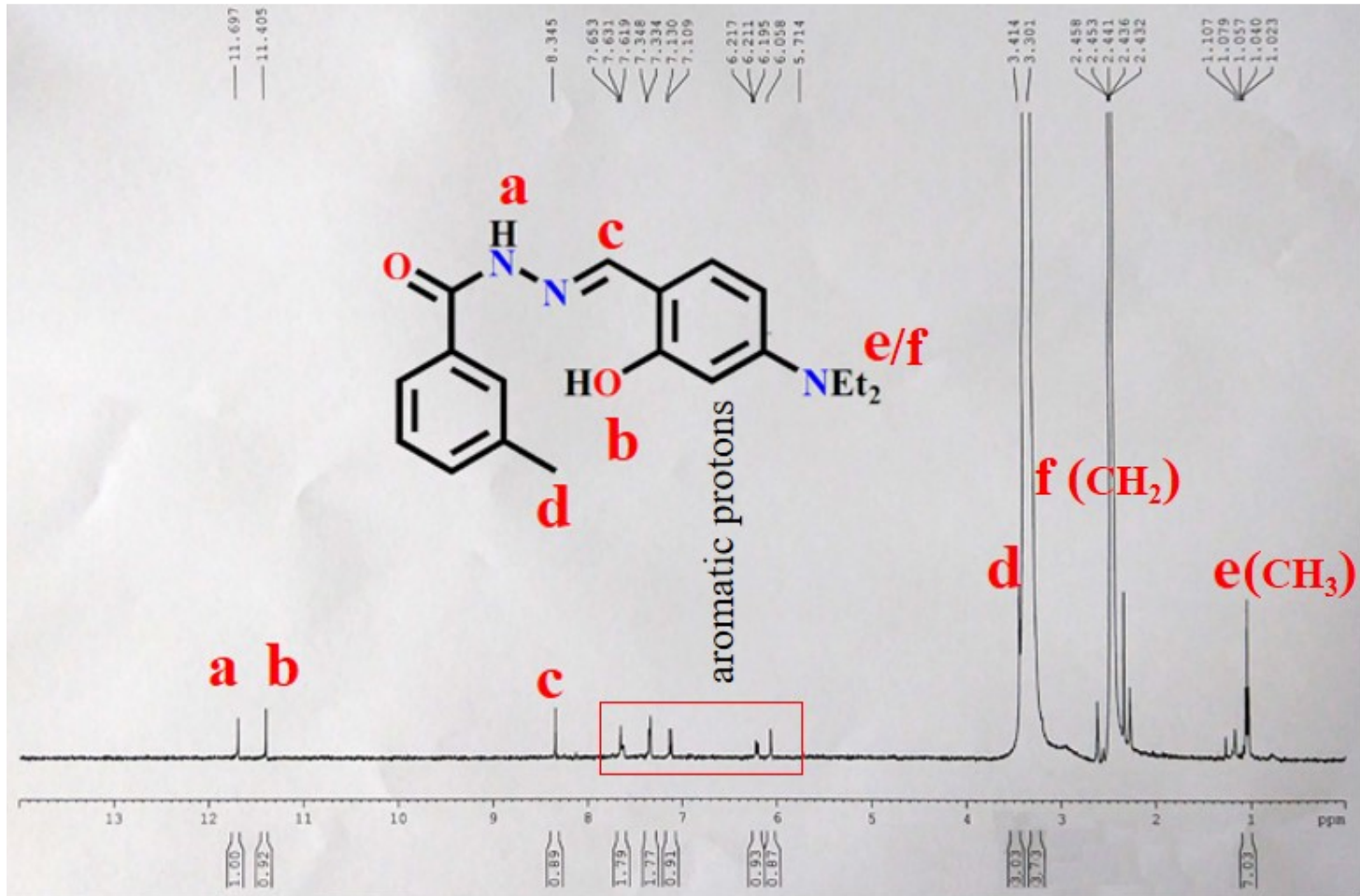


Figure S2b  $^1\text{H}$  NMR spectrum of **L1** in  $\text{DMSO}-d_6$

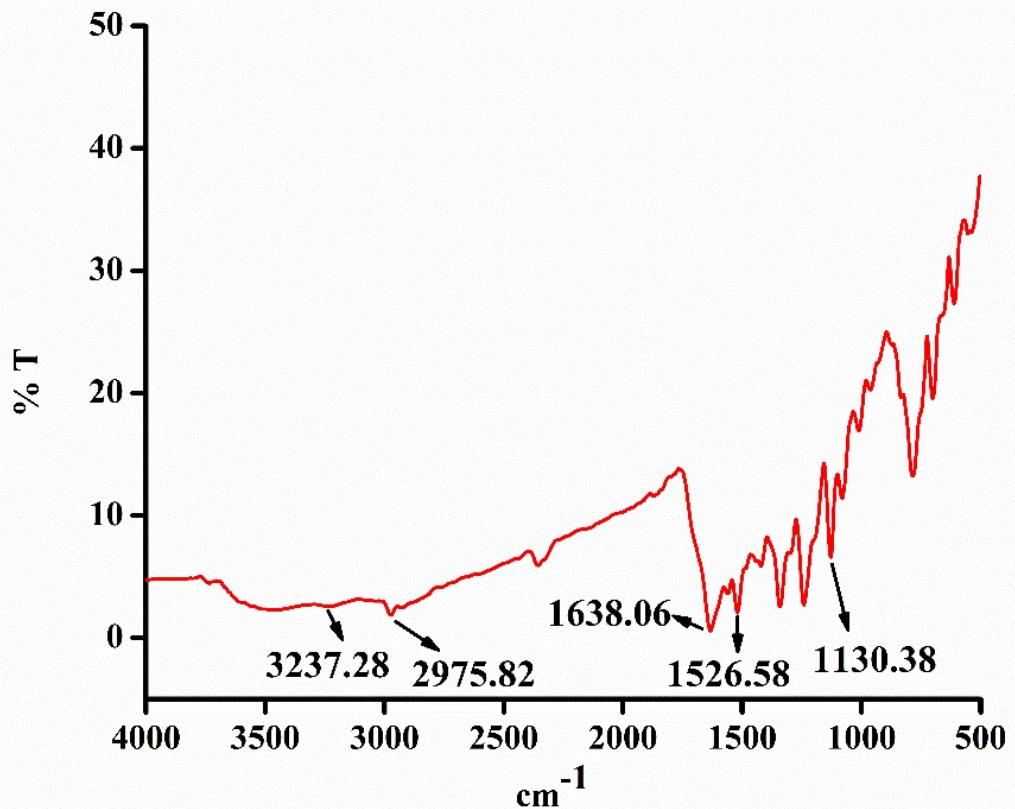
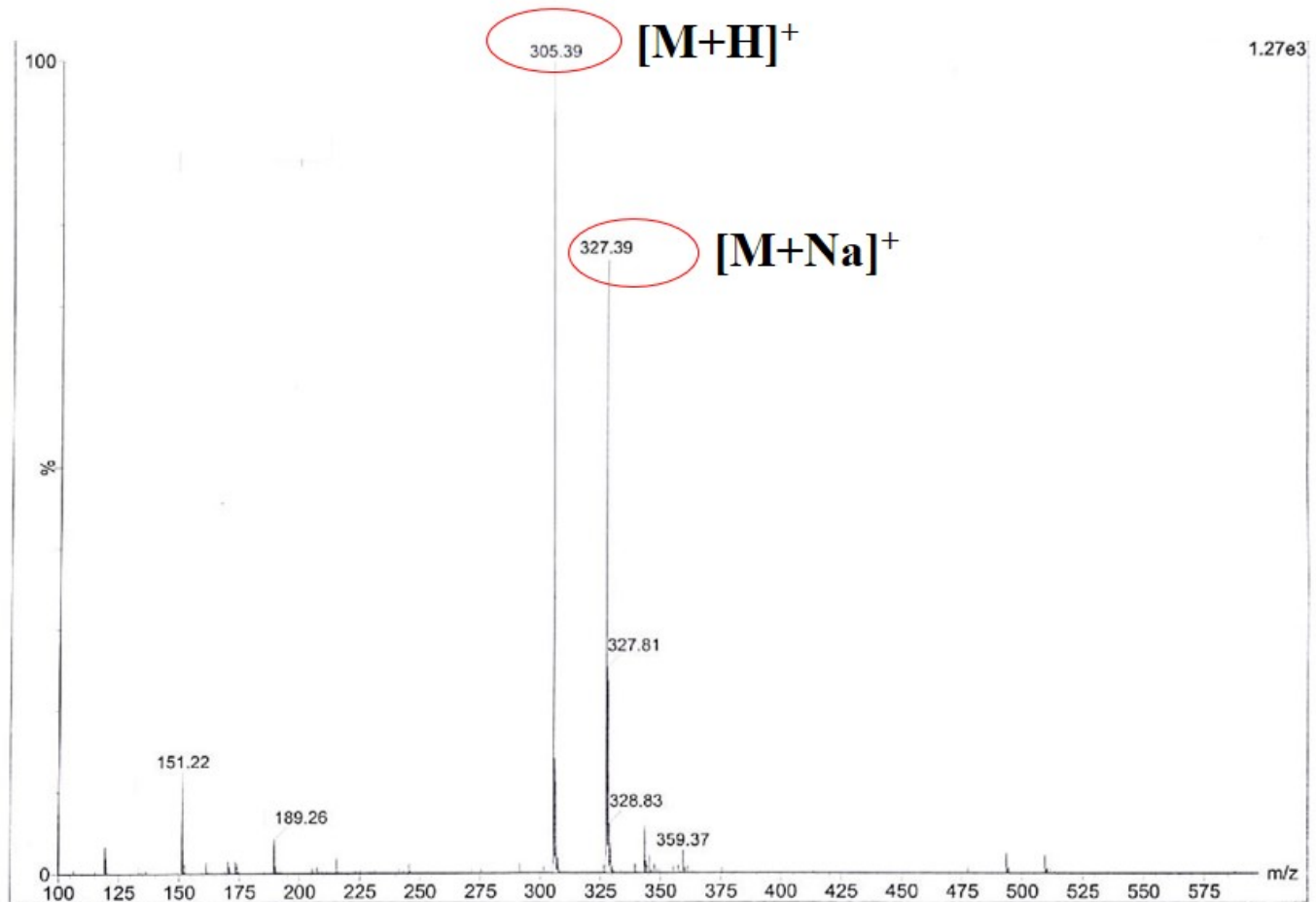
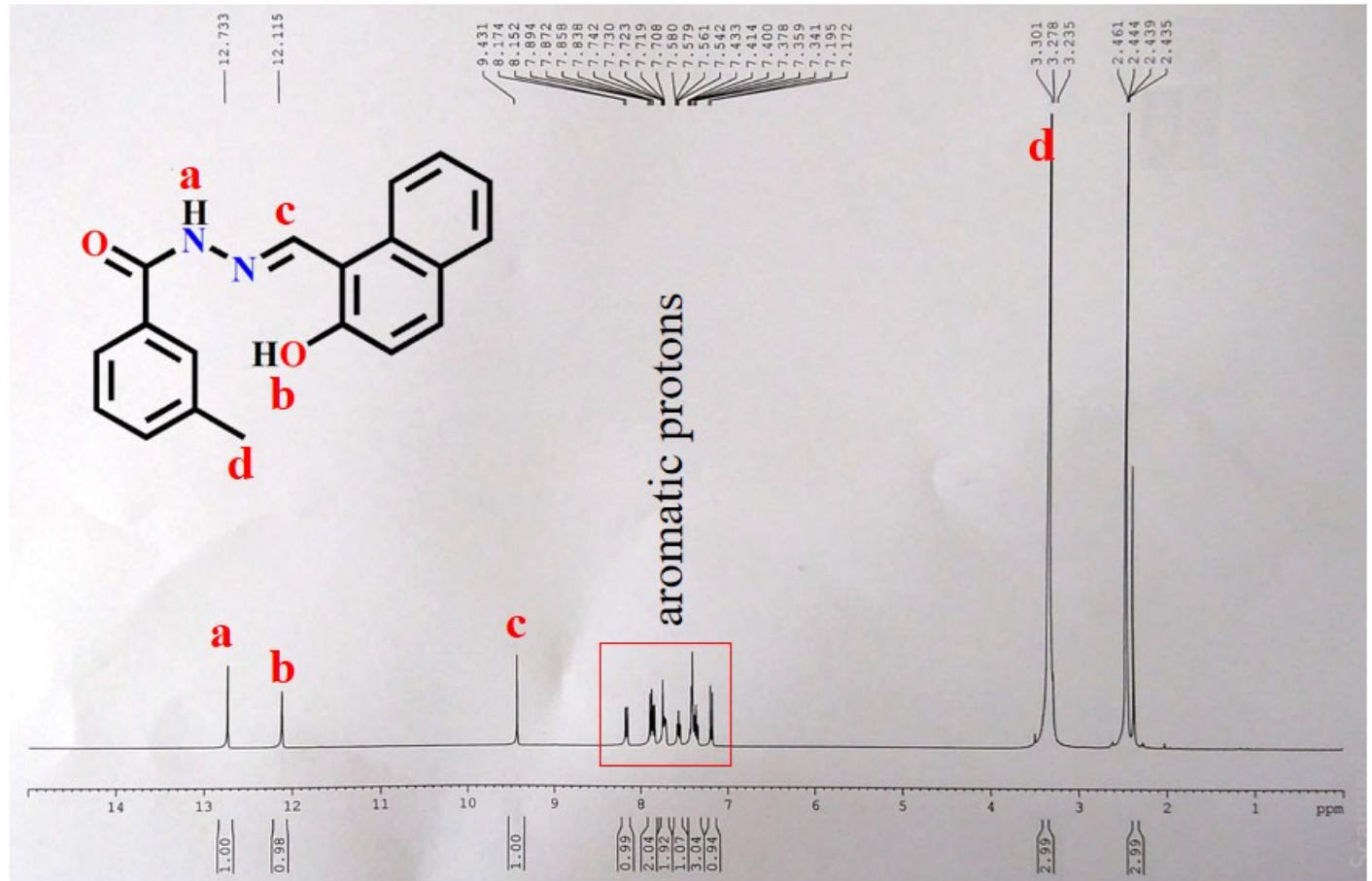


Figure S2c FTIR spectrum of **L1**



**Figure S3a** QTOF mass spectrum of L2



**Figure S3b**  $^1\text{H}$  NMR spectrum of **L2** in  $\text{DMSO}-d_6$

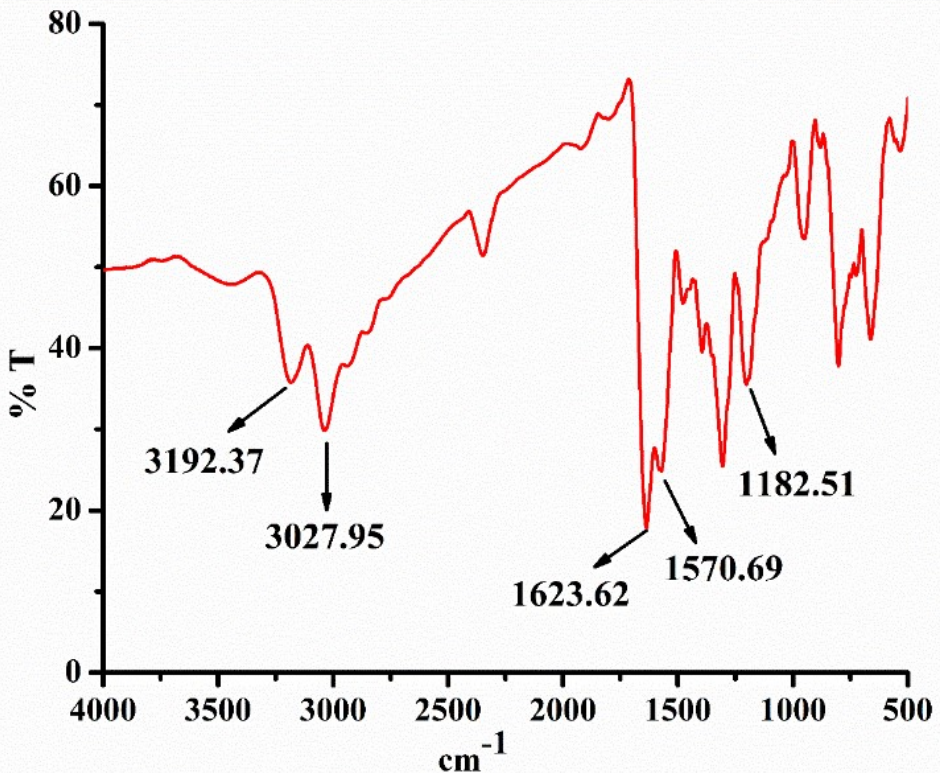
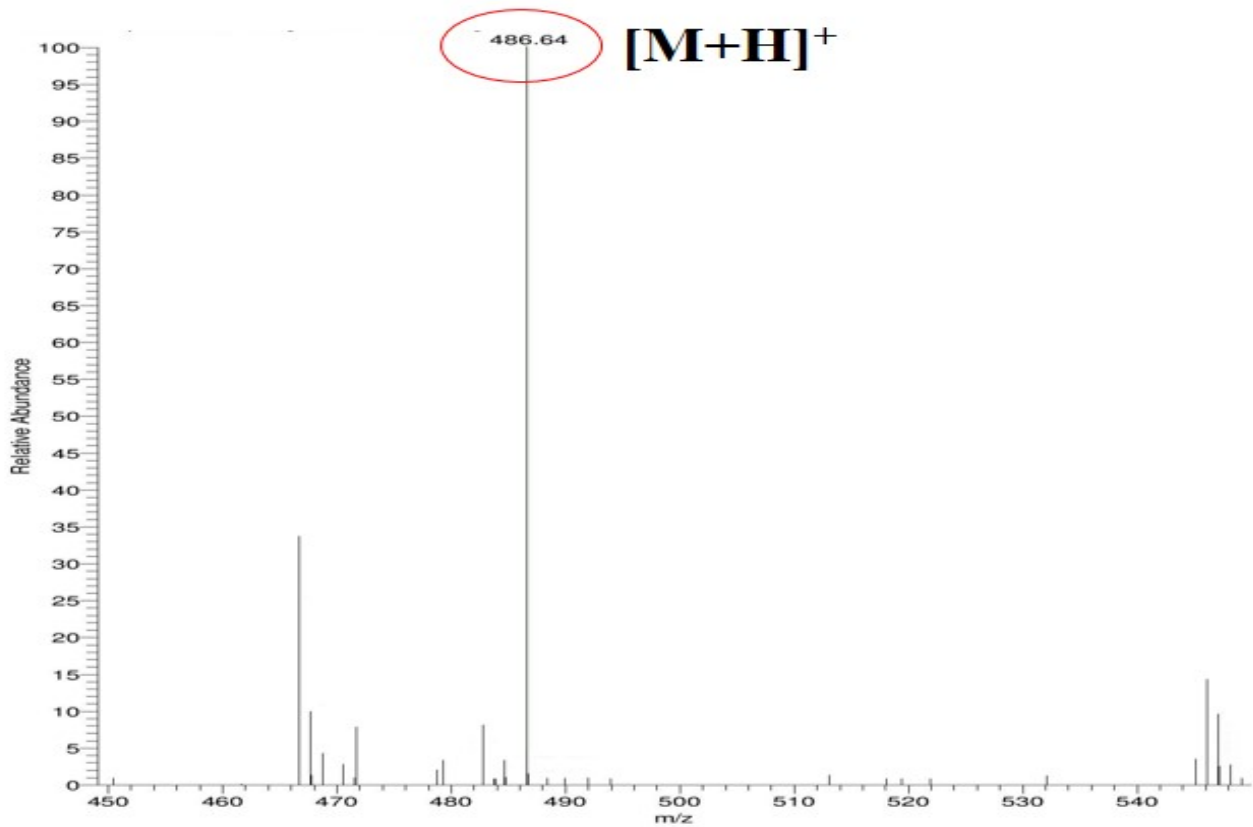
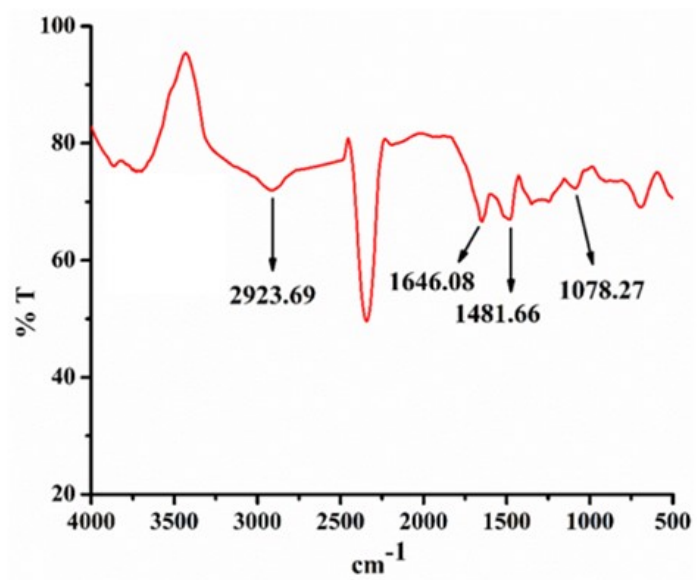


Figure S3c FTIR spectrum of L2





**Figure S4b** FTIR spectrum of **M1**

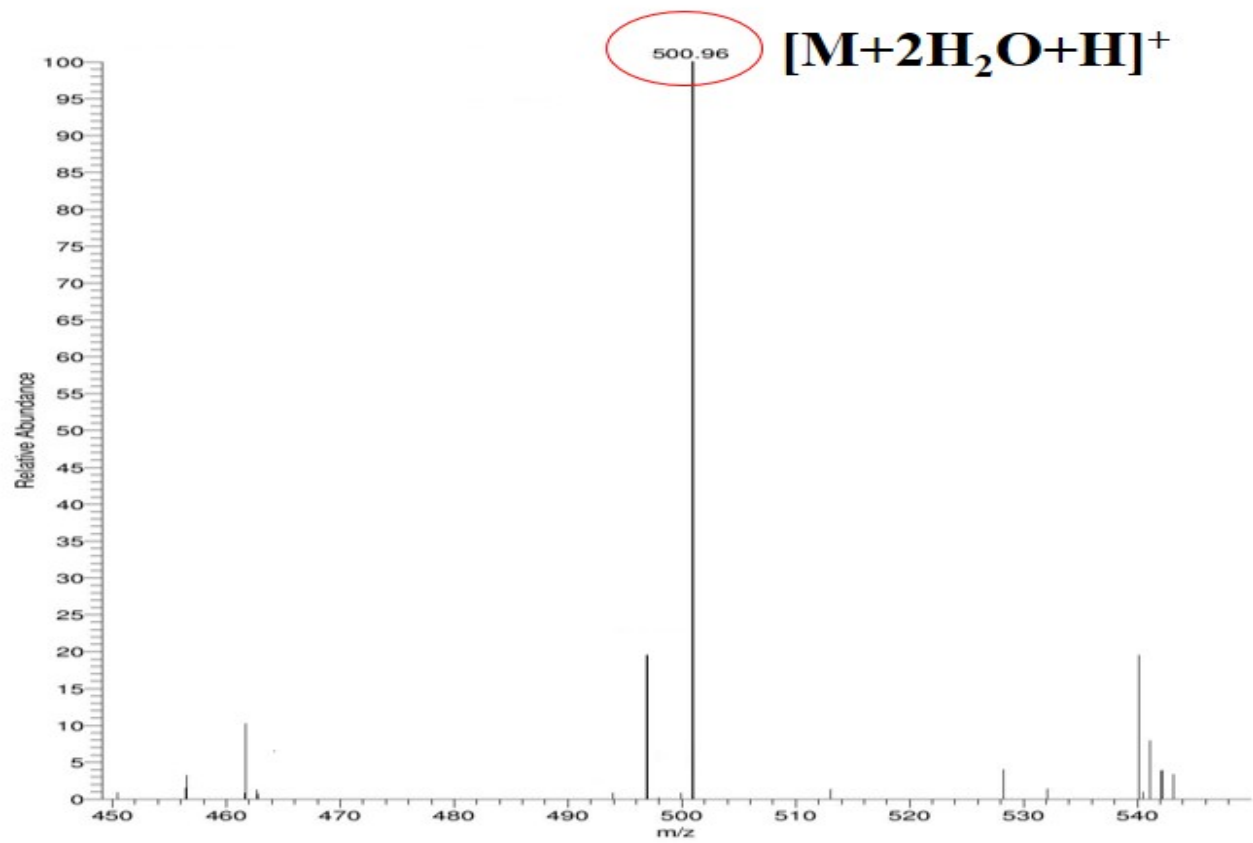


Figure S5aQTOF mass spectrum of M2

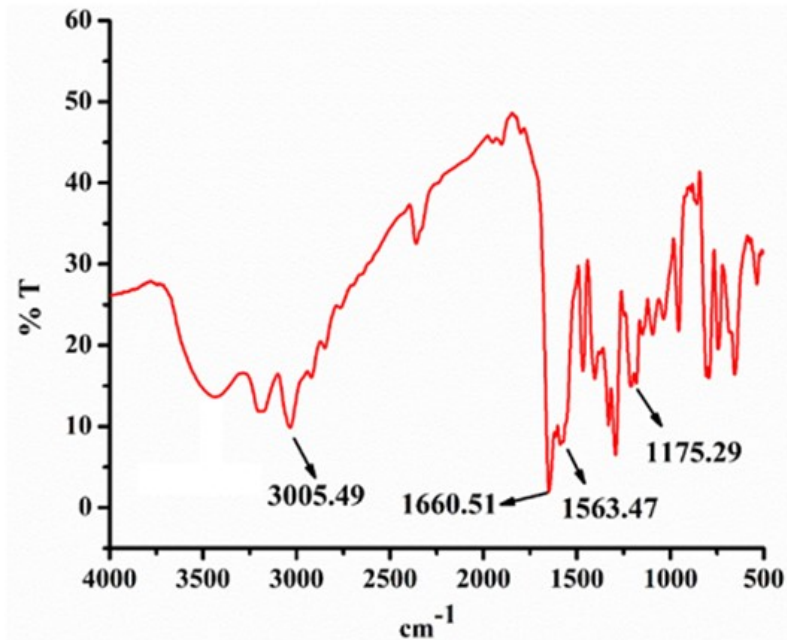


Figure S5b FTIR spectrum of M2

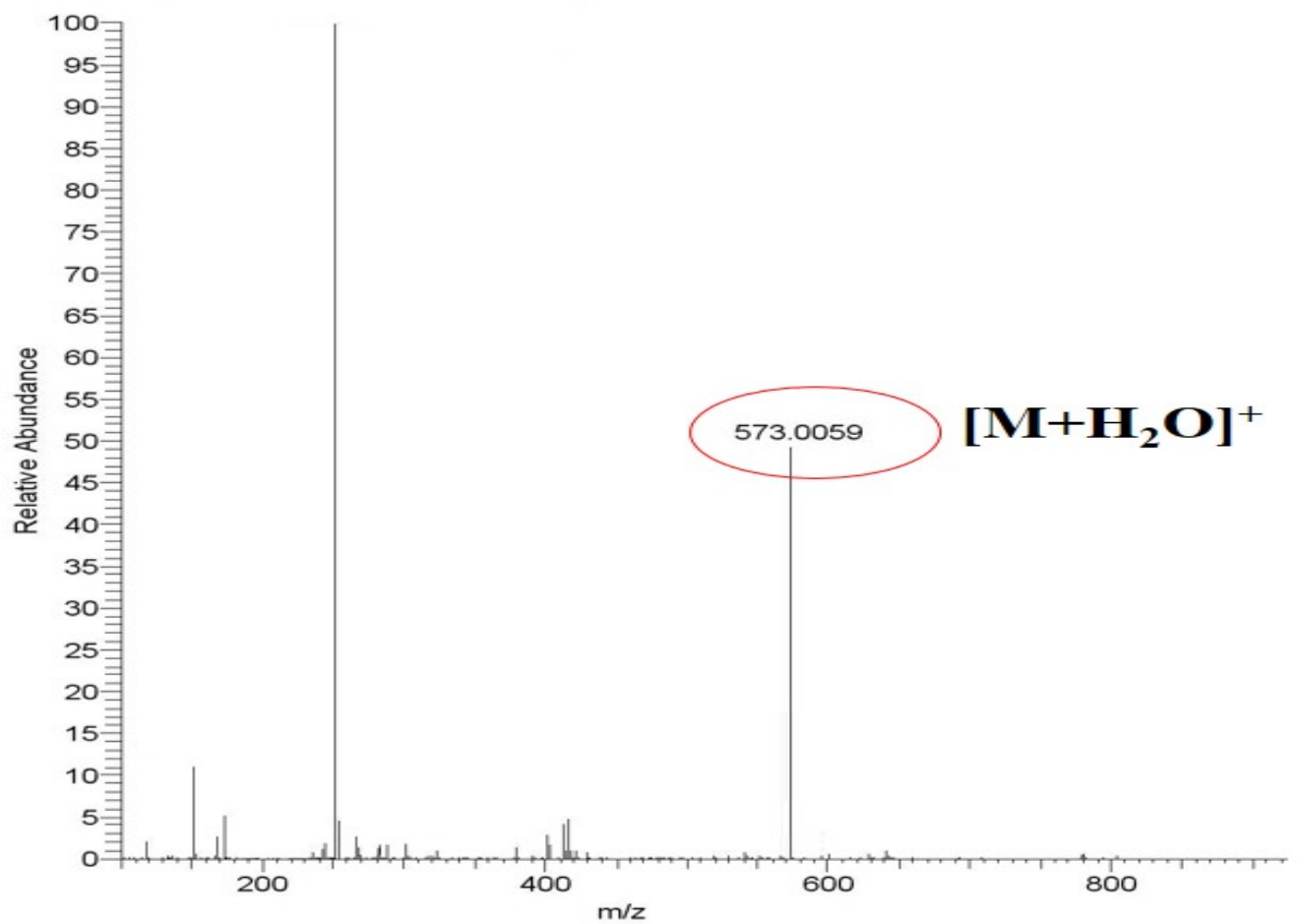
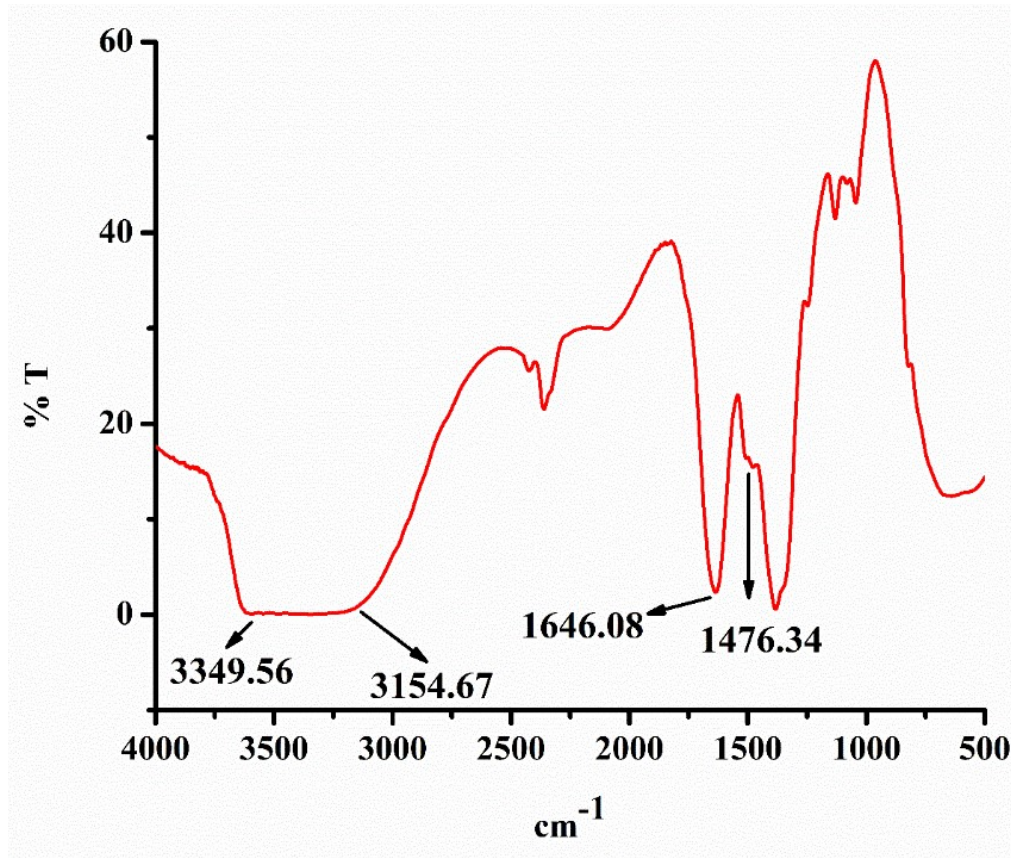


Figure S6a QTOF mass spectrum of Y1



**Figure S6b** FTIR spectrum of Y1

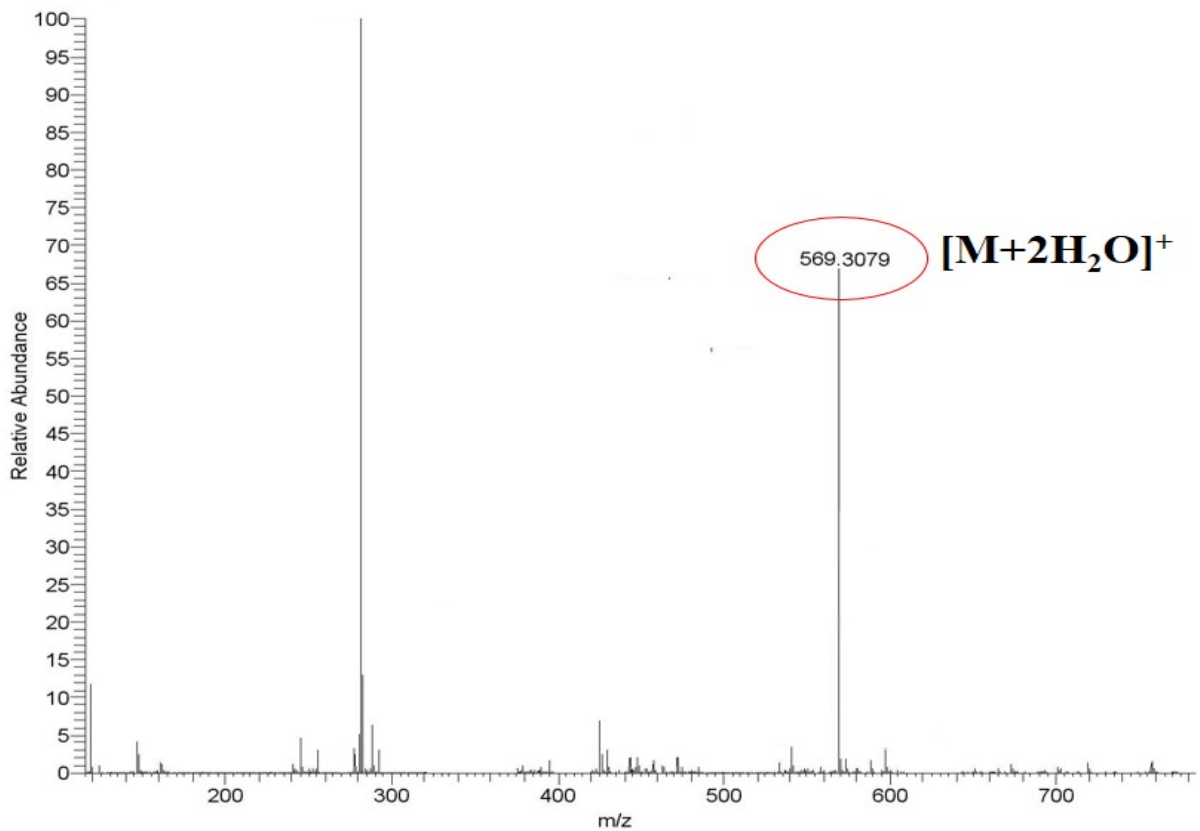


Figure S7a QTOF mass spectrum of Y2

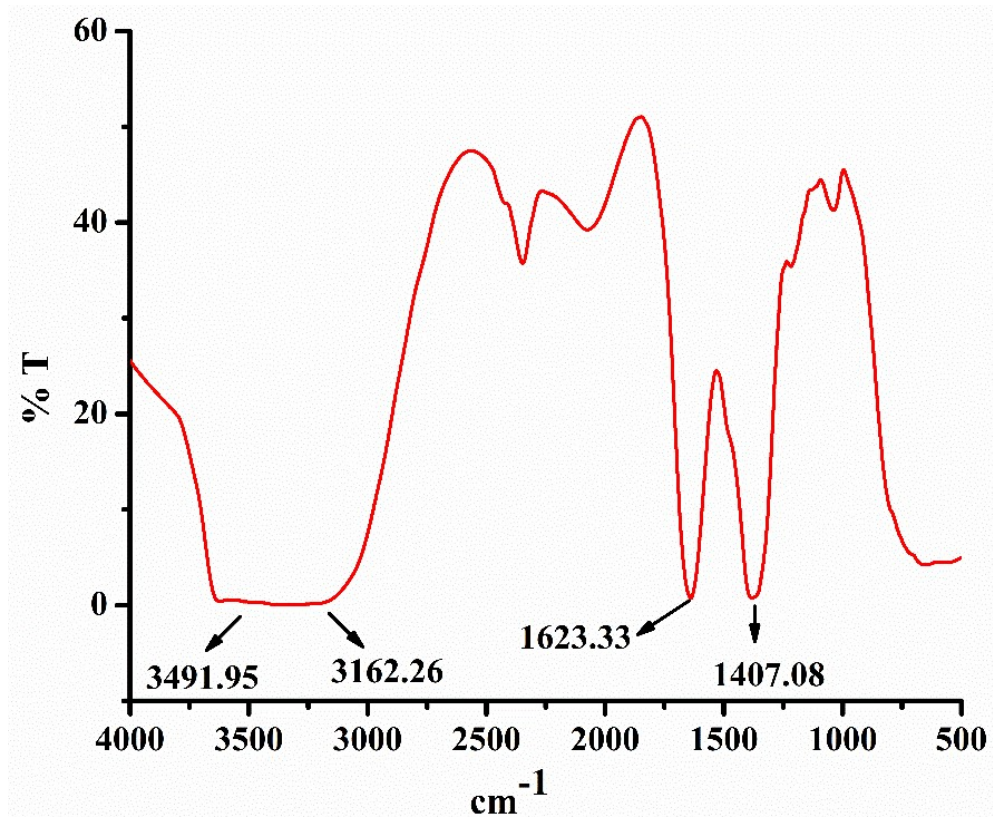
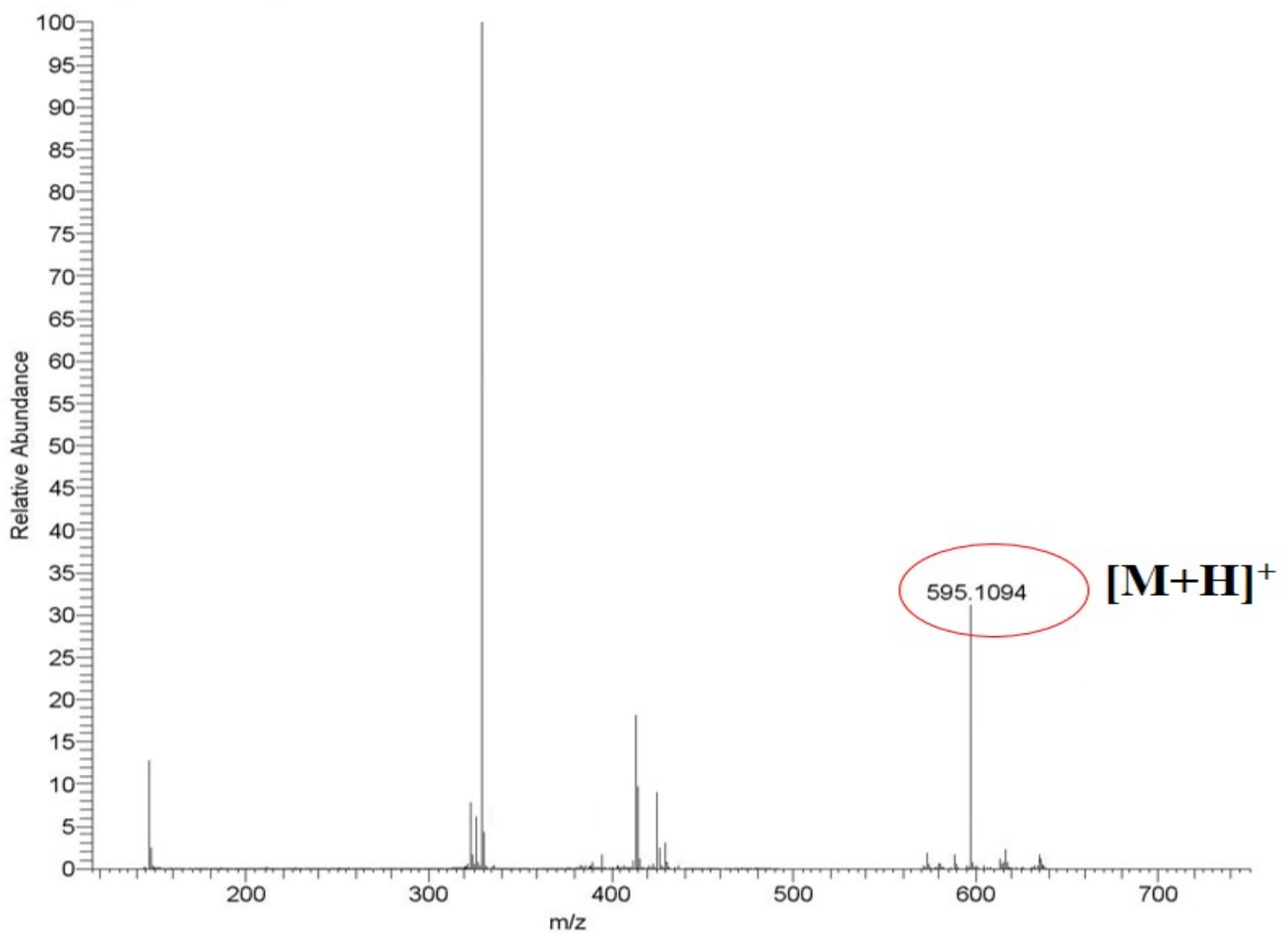


Figure S7b FTIR spectrum of Y2



**Figure S8a** QTOF mass spectrum of P1

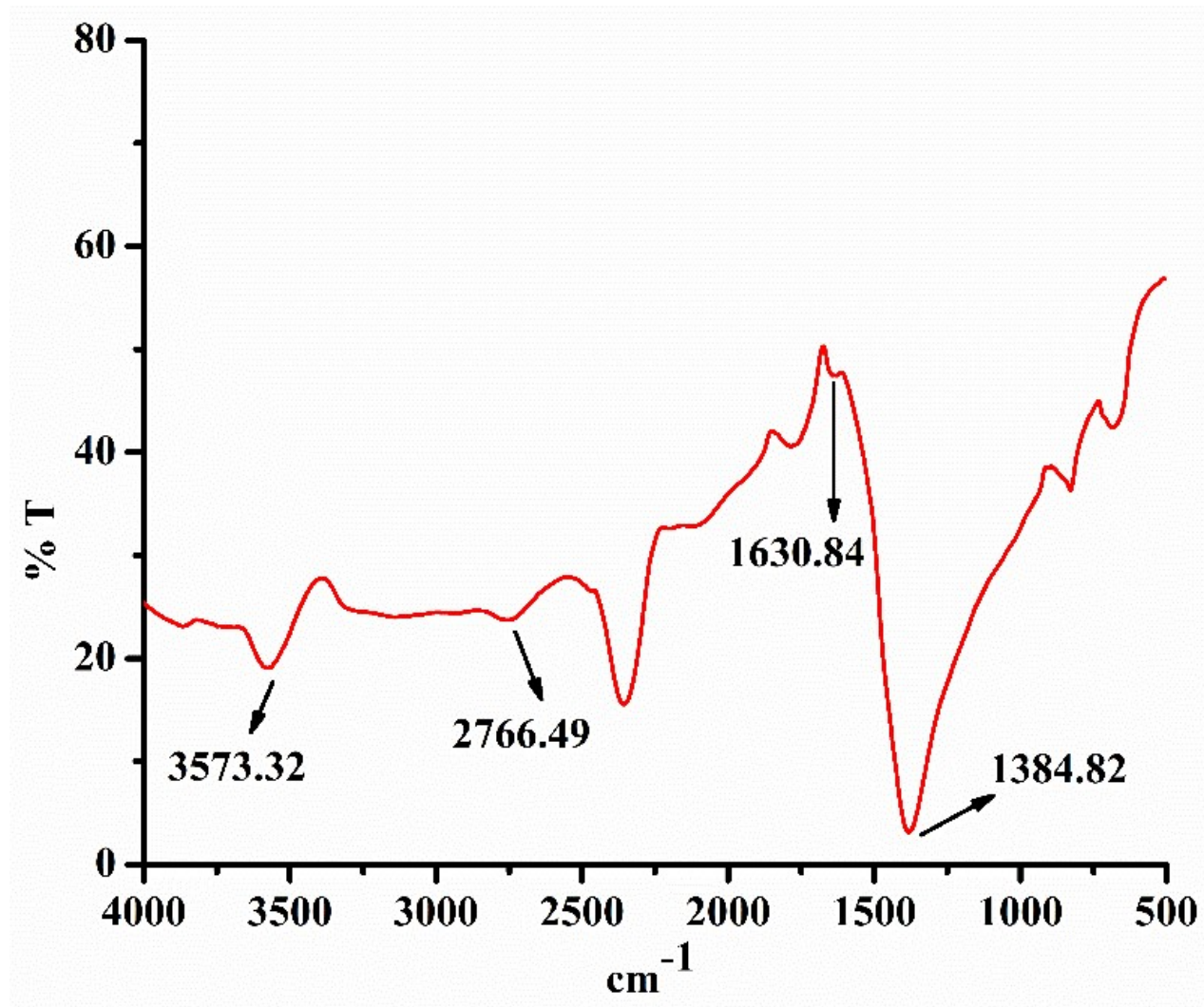
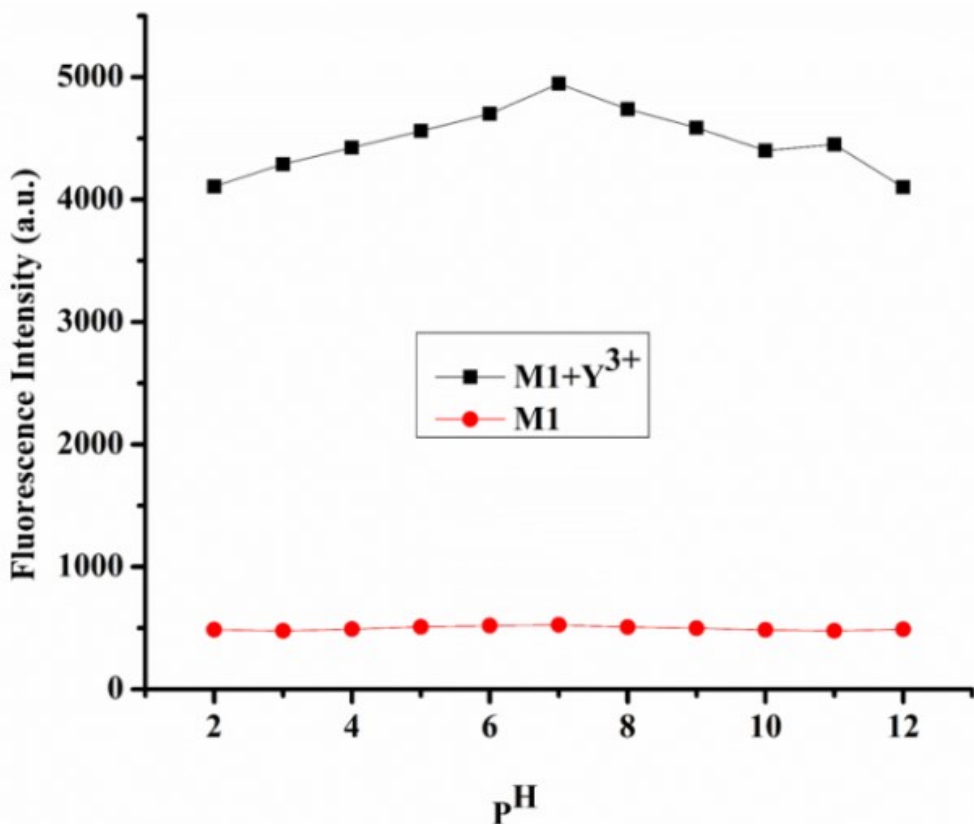
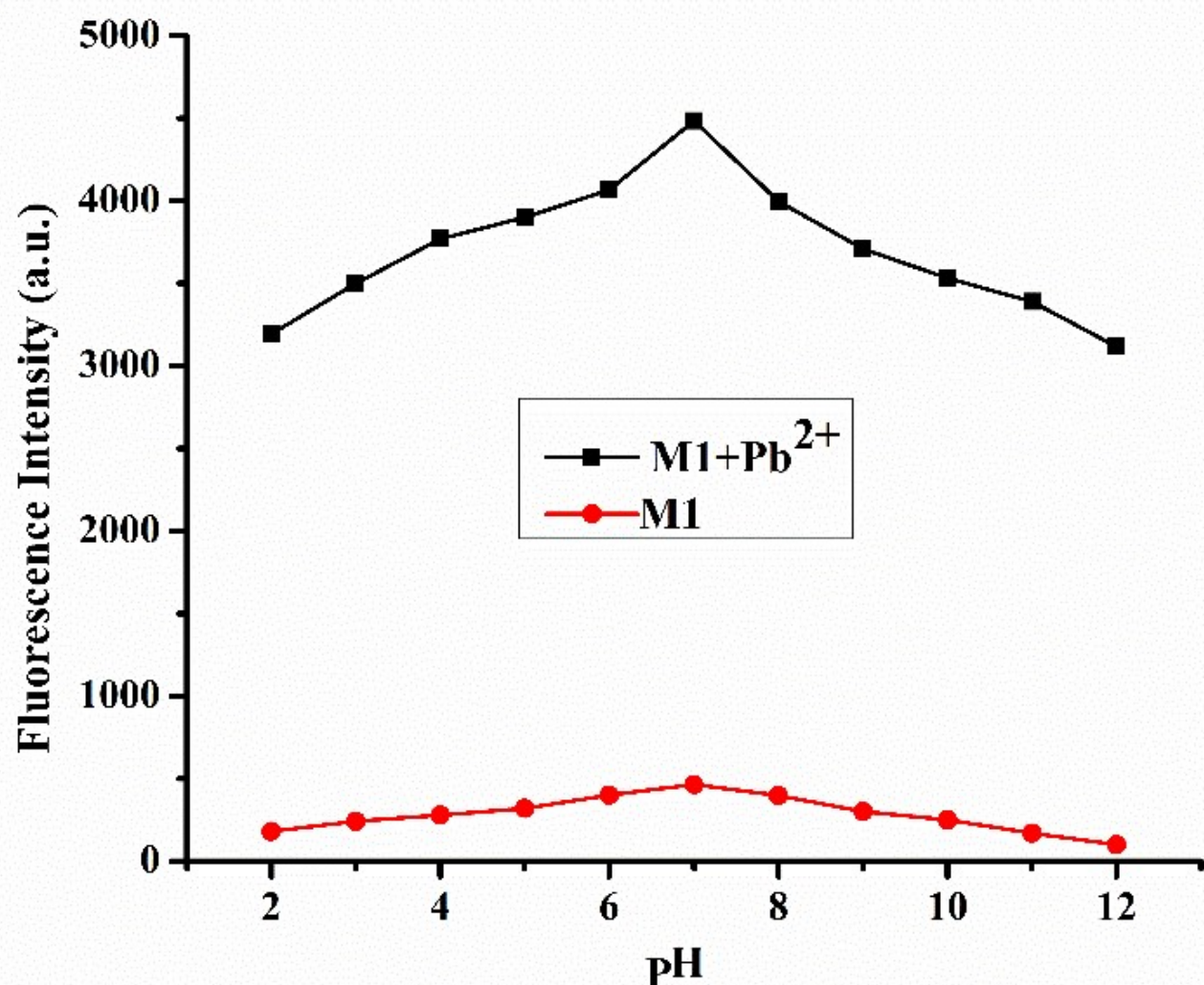


Figure S8b FTIR spectrum of P1



**Figure S9a** Effect of pH on the emission intensities of M1 ( $\lambda_{\text{ex}} = 410 \text{ nm}$ ,  $\lambda_{\text{em}} = 527 \text{ nm}$ ) in presence and absence of Y<sup>3+</sup>



**Figure S9b** Effect of pH on the emission intensities of compound **M1** ( $\lambda_{\text{ex}} = 410 \text{ nm}$ ,  $\lambda_{\text{em}} = 463 \text{ nm}$ ) in presence and absence of  $\text{Pb}^{2+}$

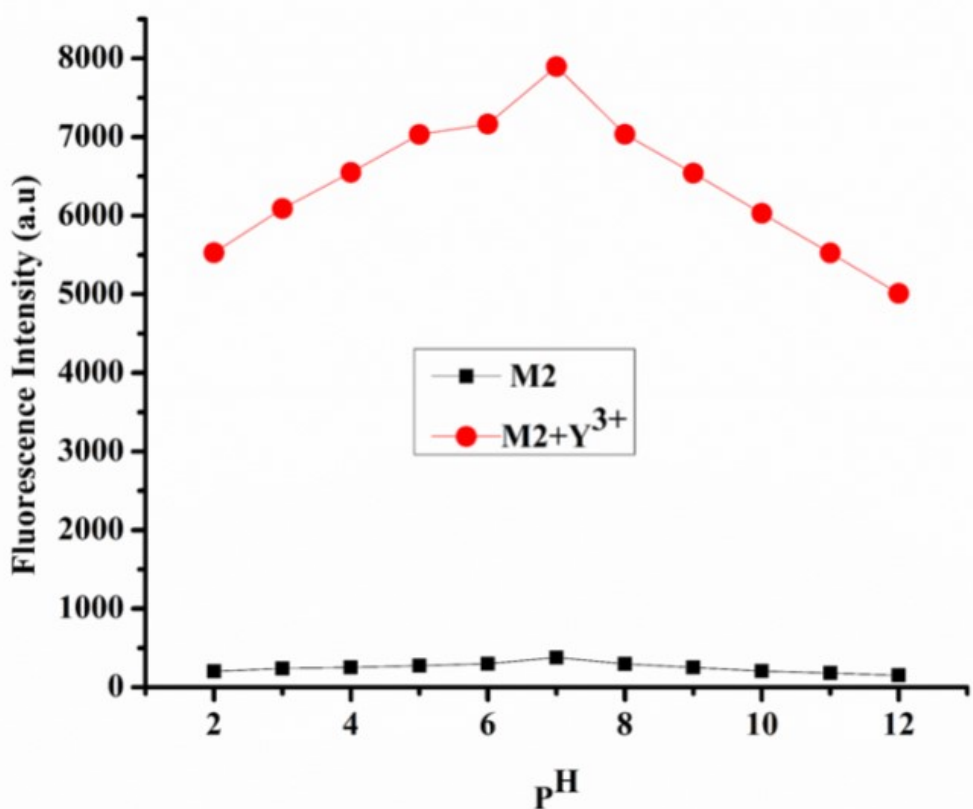


**Figure S9c** Effect of pH on the emission intensities of **M2** ( $\lambda_{\text{ex}} = 342 \text{ nm}$ ,  $\lambda_{\text{em}} = 497 \text{ nm}$ ) in presence and absence of  $\text{Y}^{3+}$

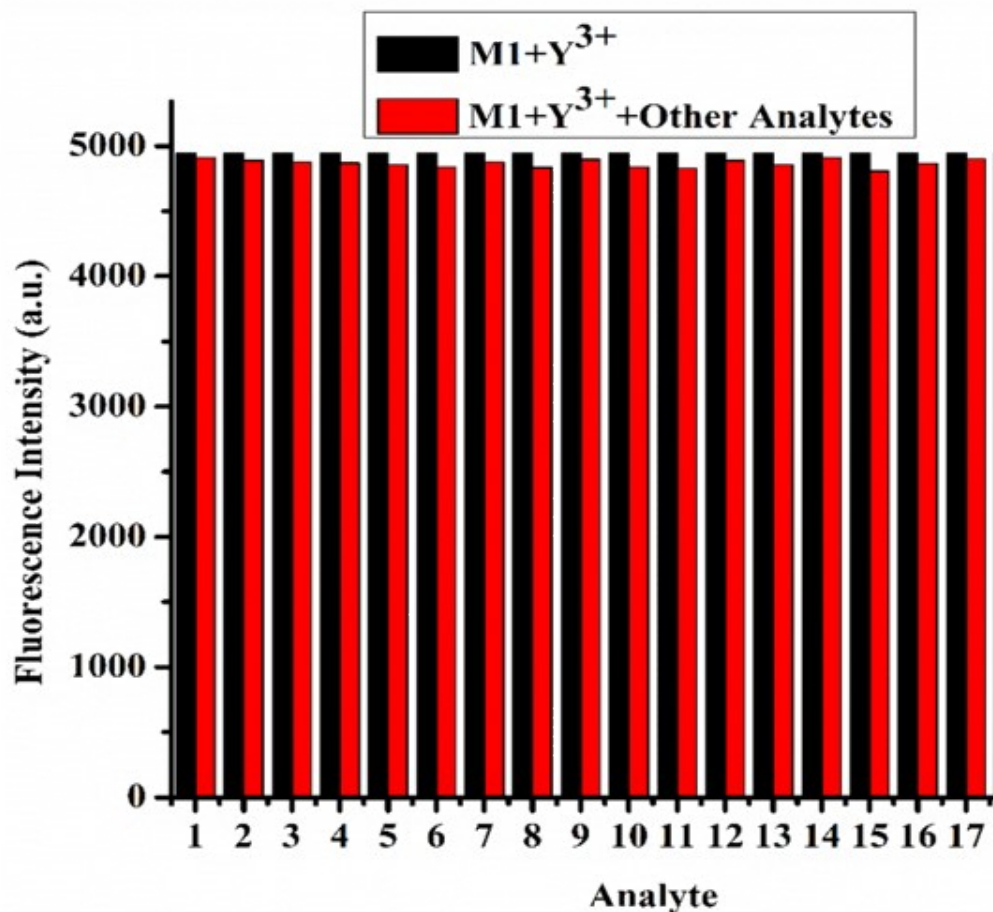


**Figure S10a** Interference plots (cations) of **M1** for  $\text{Y}^{3+}$  in fluorescence ( $\lambda_{\text{ex}} = 410 \text{ nm}$ ,  $\lambda_{\text{em}} = 527 \text{ nm}$ ). 1;  $\text{Cu}^{2+}$ , 2;  $\text{Cr}^{3+}$ , 3;  $\text{Mn}^{2+}$ , 4;  $\text{Fe}^{2+}$ , 5;  $\text{Fe}^{3+}$ , 6;  $\text{Co}^{2+}$ , 7;  $\text{Ni}^{2+}$ , 8;  $\text{Al}^{3+}$ , 9;  $\text{Zn}^{2+}$ , 10;  $\text{Ag}^+$ , 11;  $\text{Cd}^{2+}$ , 12;  $\text{Hg}^{2+}$ , 13;  $\text{La}^{3+}$ , 14;  $\text{Ce}^{4+}$ , 15;  $\text{Gd}^{3+}$ , 16;  $\text{Tb}^{3+}$ , and 17;  $\text{Dy}^{3+}$

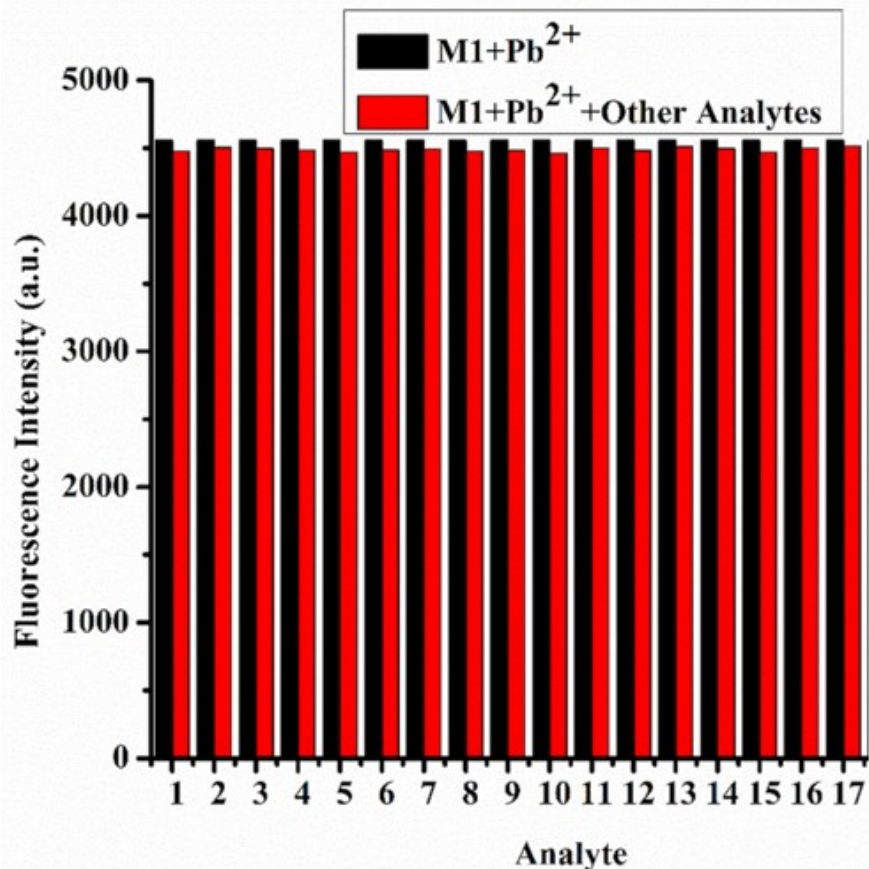


**Figure S10b** Interference plots (cations) of **M1** for  $\text{Pb}^{2+}$  in fluorescence ( $\lambda_{\text{ex}} = 410$  nm,  $\lambda_{\text{em}} = 463$  nm). 1;  $\text{Cu}^{2+}$ , 2;  $\text{Cr}^{3+}$ , 3;  $\text{Mn}^{2+}$ , 4;  $\text{Fe}^{2+}$ , 5;  $\text{Fe}^{3+}$ , 6;  $\text{Co}^{2+}$ , 7;  $\text{Ni}^{2+}$ , 8;  $\text{Al}^{3+}$ , 9;  $\text{Zn}^{2+}$ , 10;  $\text{Ag}^{+}$ , 11;  $\text{Cd}^{2+}$ , 12;  $\text{Hg}^{2+}$ , 13;  $\text{La}^{3+}$ , 14;  $\text{Ce}^{4+}$ , 15;  $\text{Gd}^{3+}$ , 16;  $\text{Tb}^{3+}$  and 17;  $\text{Dy}^{3+}$

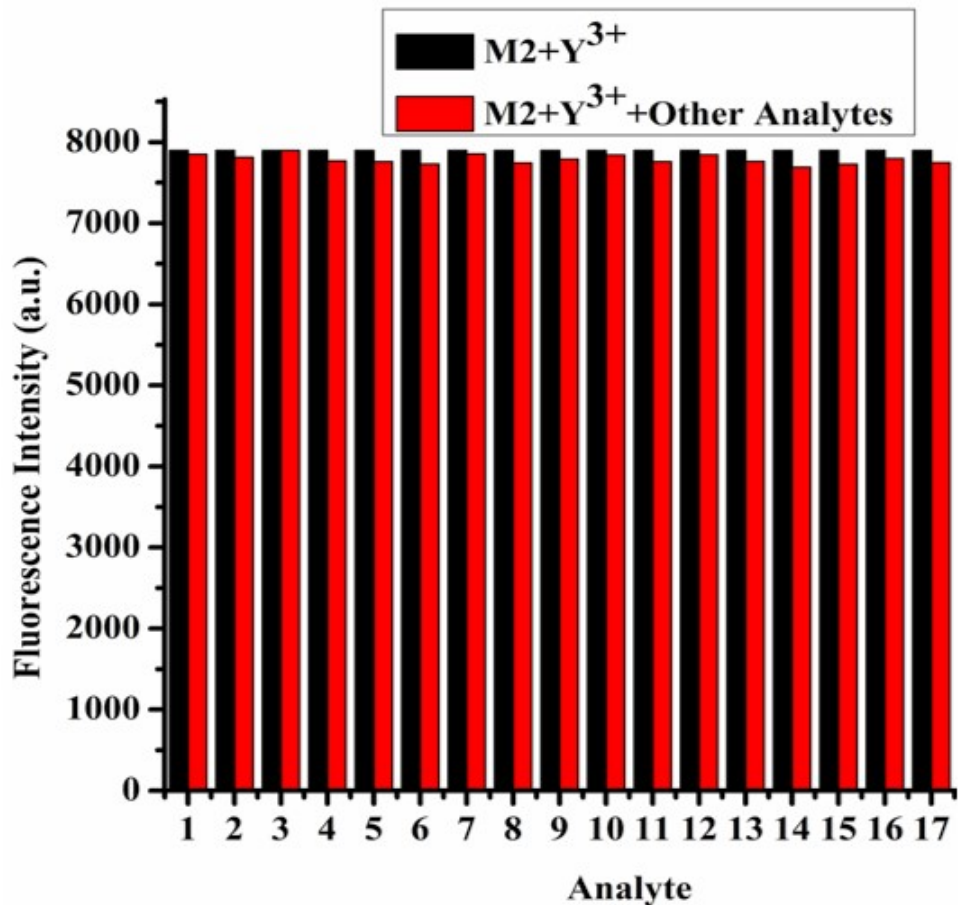


**Figure S10c** Interference plots (cations) of **M2** for  $\text{Y}^{3+}$  in fluorescence ( $\lambda_{\text{ex}} = 342 \text{ nm}$ ,  $\lambda_{\text{em}} = 497 \text{ nm}$ ). . 1;  $\text{Cu}^{2+}$ , 2;  $\text{Cr}^{3+}$ , 3;  $\text{Mn}^{2+}$ , 4;  $\text{Fe}^{2+}$ , 5;  $\text{Fe}^{3+}$ , 6;  $\text{Co}^{2+}$ , 7;  $\text{Ni}^{2+}$ , 8;  $\text{Al}^{3+}$ , 9;  $\text{Zn}^{2+}$ , 10;  $\text{Ag}^+$ , 11;  $\text{Cd}^{2+}$ , 12;  $\text{Hg}^{2+}$ , 13;  $\text{La}^{3+}$ , 14;  $\text{Ce}^{4+}$ , 15;  $\text{Gd}^{3+}$ , 16;  $\text{Tb}^{3+}$  and 17;  $\text{Dy}^{3+}$

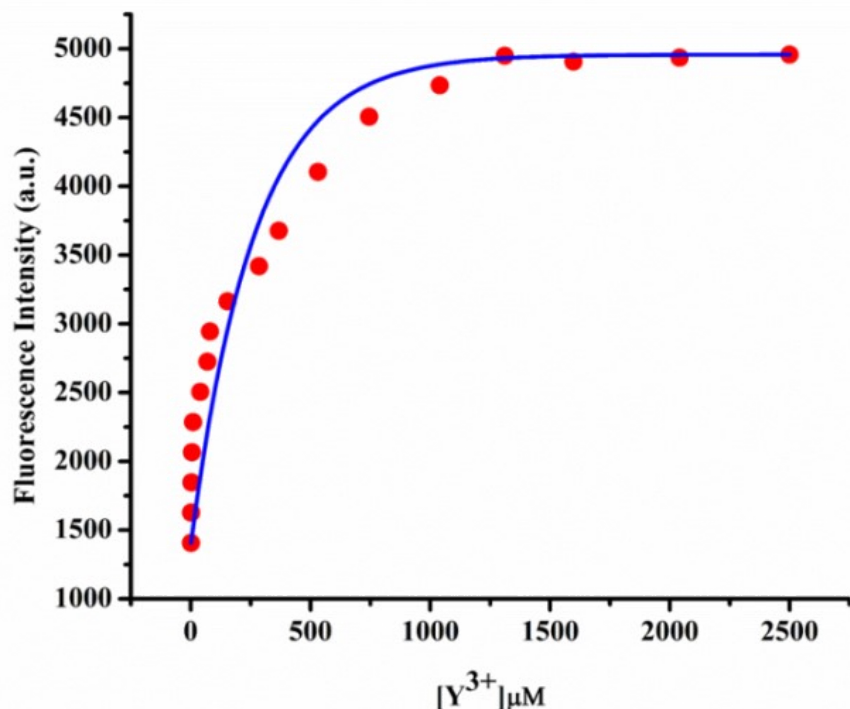


**Figure S11a** Plot of emission intensities of **M1** ( $20 \mu\text{M}$ ,  $\lambda_{\text{ex}} = 410 \text{ nm}$ ,  $\lambda_{\text{em}} = 527 \text{ nm}$ ) as a function of externally added  $\text{Y}^{3+}$ ( $1.0\text{-}2500 \mu\text{M}$ )

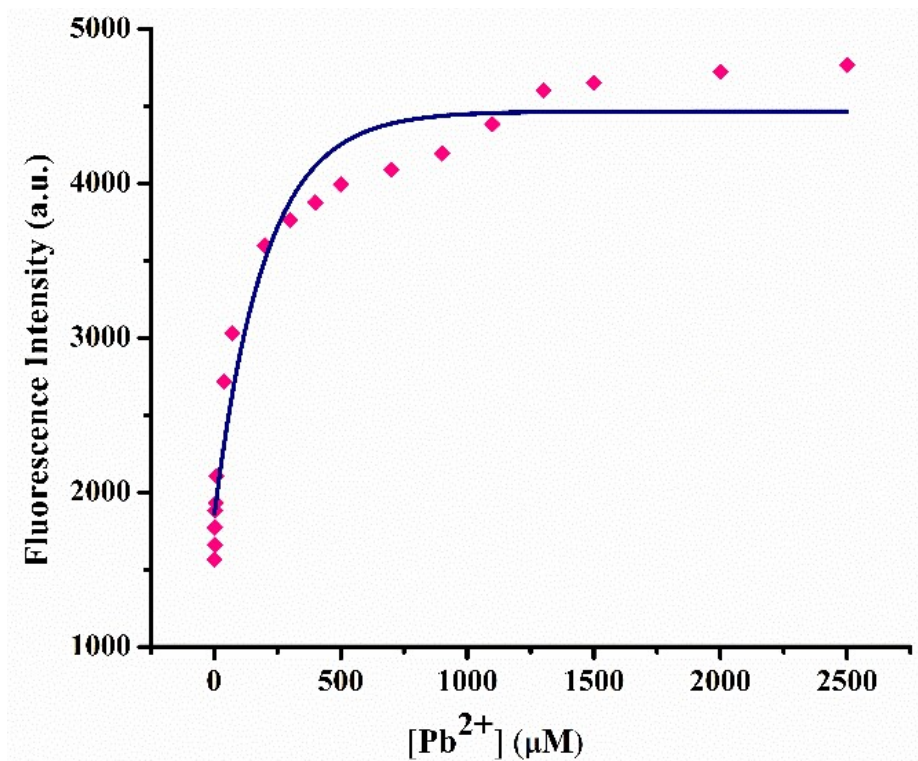


**Figure S11b** Plot of emission intensities of **M1** ( $20 \mu\text{M}$ ,  $\lambda_{\text{ex}} = 410 \text{ nm}$ ,  $\lambda_{\text{em}} = 463 \text{ nm}$ ) as a function of externally added  $\text{Pb}^{2+}$ ( $1.0\text{-}2500 \mu\text{M}$ ).

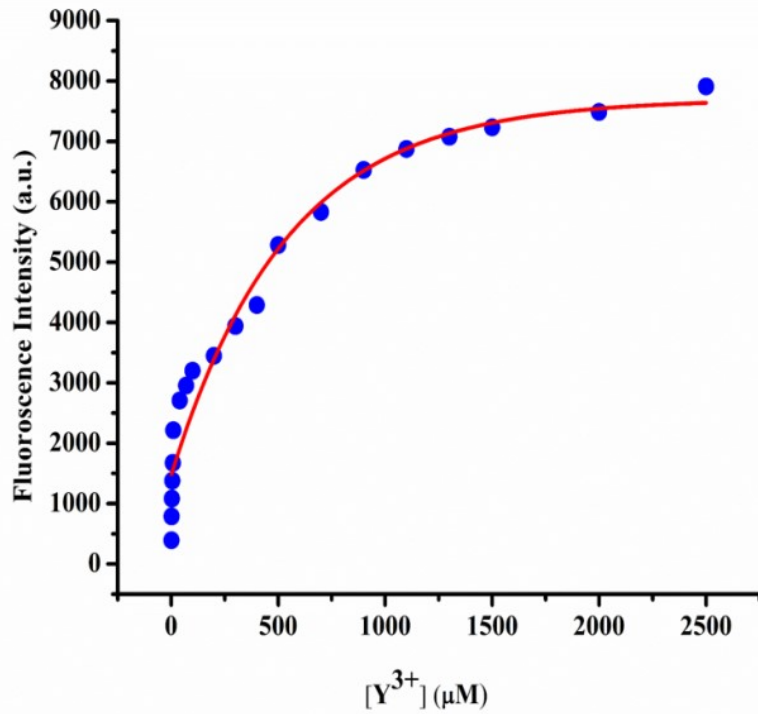


**Figure S11c** Plot of emission intensities of **M2** ( $20 \mu\text{M}$ ,  $\lambda_{\text{ex}} = 342 \text{ nm}$ ,  $\lambda_{\text{em}} = 497 \text{ nm}$ ) as a function of externally added  $\text{Y}^{3+}$  ( $1.0$ - $2500 \mu\text{M}$ )

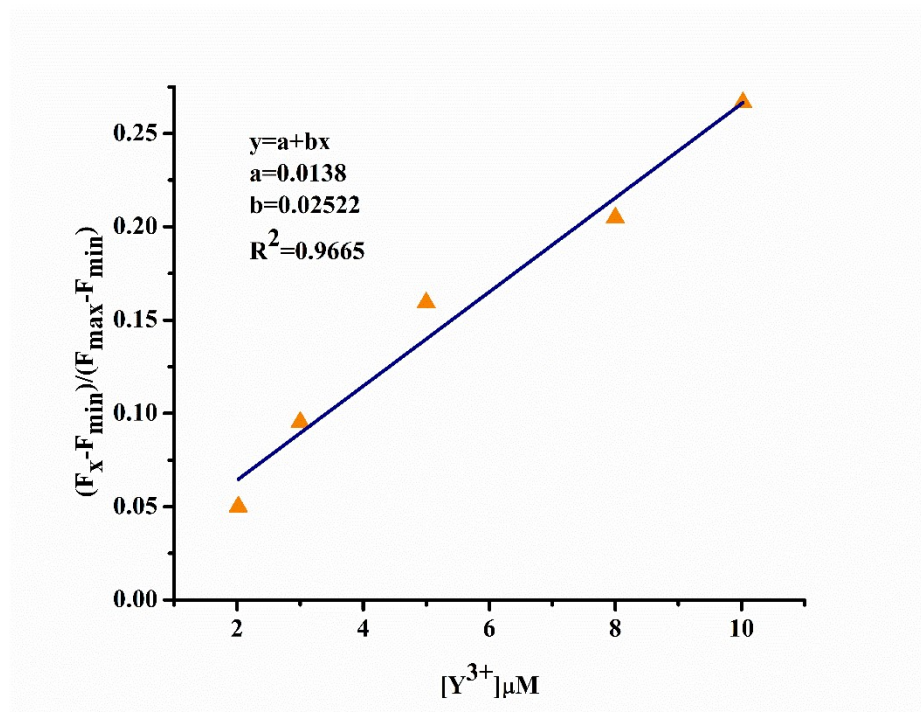


**Figure S12a** Determination of the detection limit based on change in the ratio ( $\lambda_{\text{ex}} = 410\text{nm}$ ,  $\lambda_{\text{em}} = 527\text{nm}$ ) of **M1** ( $20 \mu\text{M}$ ) with  $\text{Y}^{3+}$

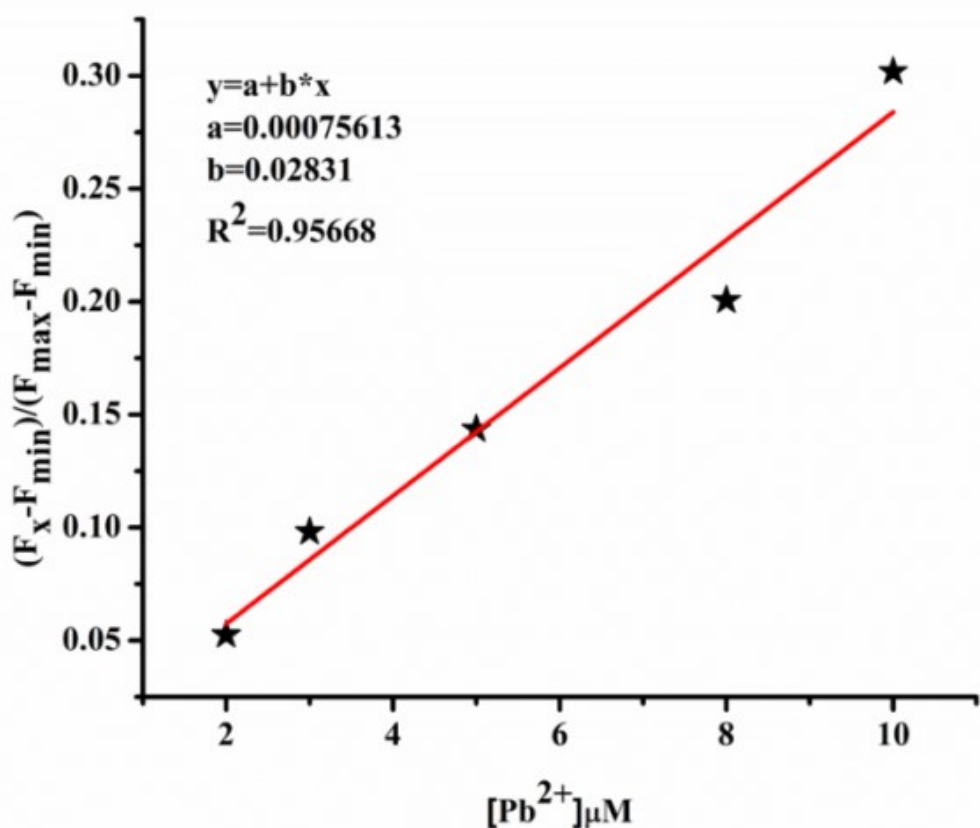


**Figure S12b** Determination of the detection limit based on change in the ratio ( $\lambda_{\text{ex}} = 410\text{nm}$ ,  $\lambda_{\text{em}} = 463\text{nm}$ ) of **M1** (20  $\mu\text{M}$ ) with  $\text{Pb}^{2+}$

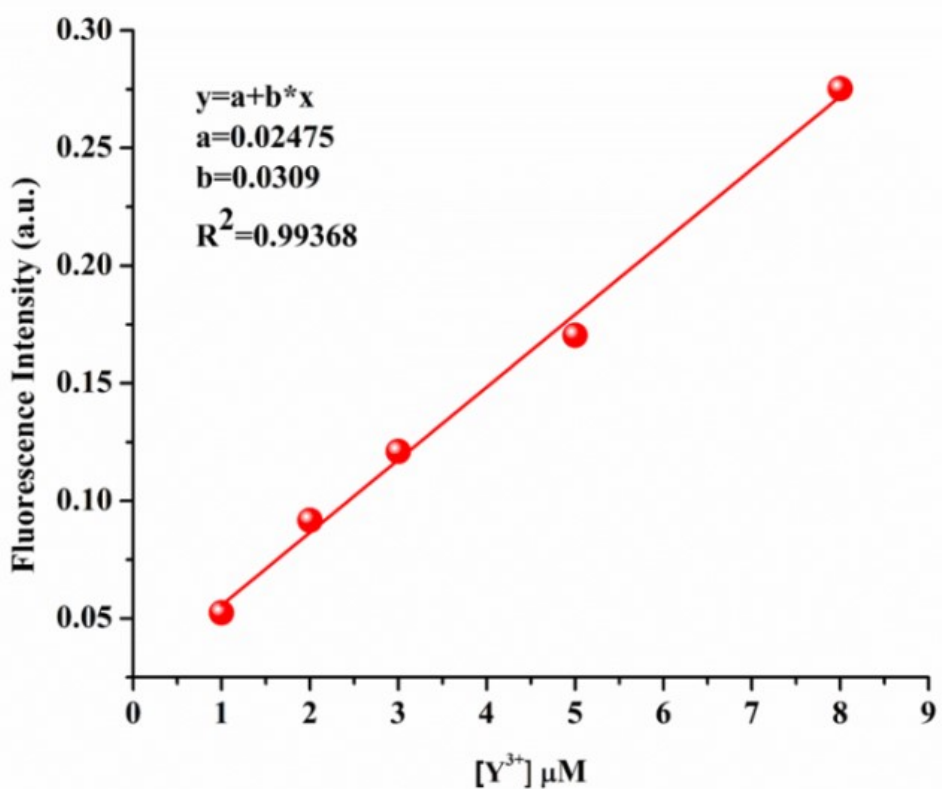


**Figure S12c** Determination of the detection limit based on change in the ratio ( $\lambda_{ex} = 342\text{nm}$ ,  $\lambda_{em} = 497\text{nm}$ ) of **M2** (20  $\mu\text{M}$ ) with  $\text{Y}^{3+}$

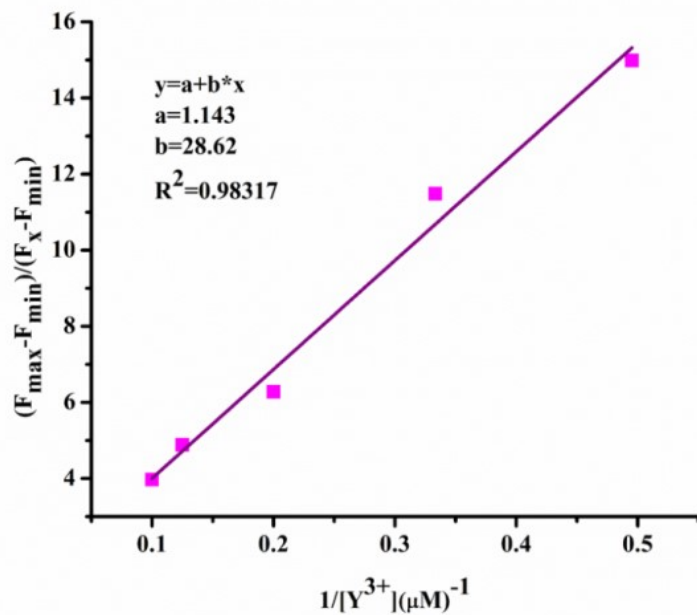


**Figure S13a** Benesi–Hildebrand plot for determination of association constant of **M1** with  $\text{Y}^{3+}$ (liner portion only)( $\lambda_{ex} = 410 \text{ nm}$ ,  $\lambda_{em} = 527\text{nm}$ )

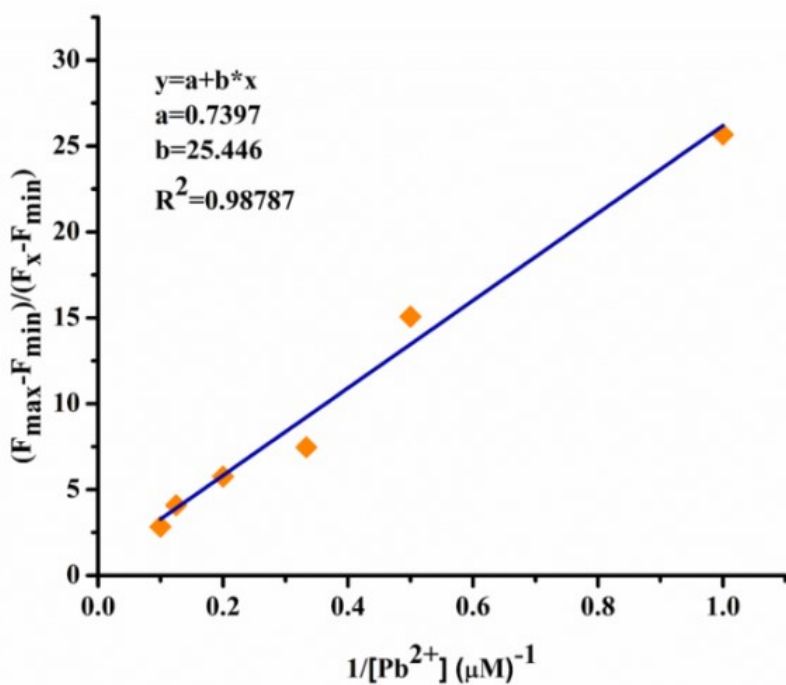


**Figure S13b** Benesi–Hildebrand plot for determination of association constant of **M1** with  $\text{Pb}^{2+}$ (liner portion only)( $\lambda_{\text{ex}} = 410 \text{ nm}$ ,  $\lambda_{\text{em}} = 463 \text{ nm}$ )

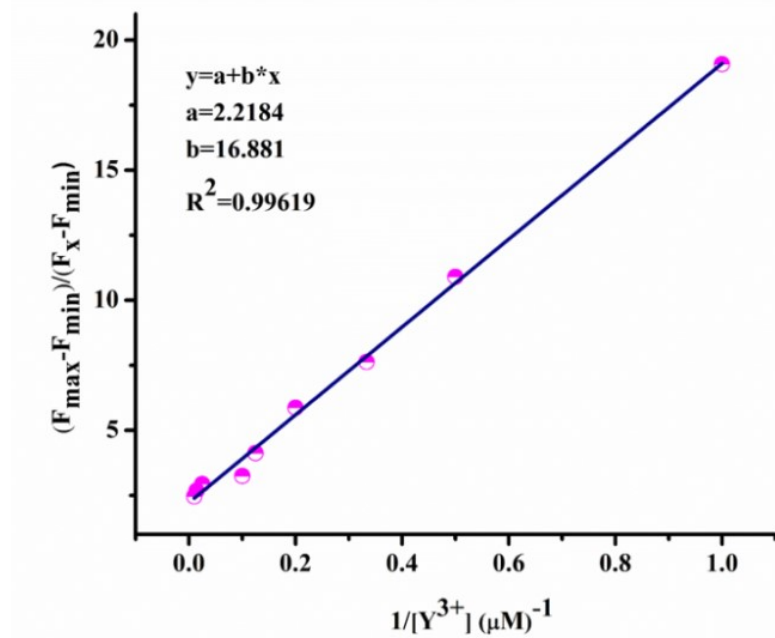


**Figure S13c** Benesi–Hildebrand plot for determination of association constant of **M2** with  $\text{Y}^{3+}$ (liner portion only)( $\lambda_{\text{ex}} = 342 \text{ nm}$ ,  $\lambda_{\text{em}} = 497 \text{ nm}$ )

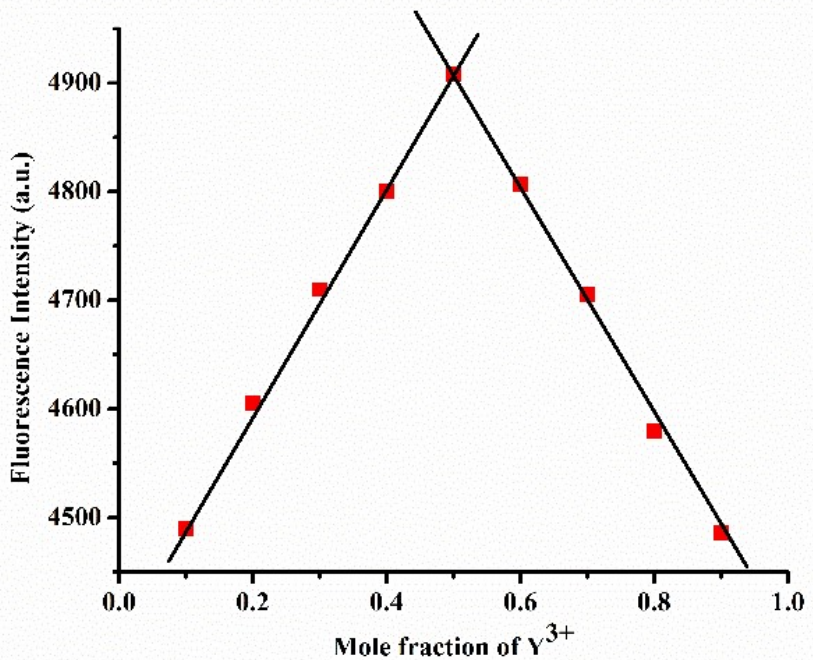


**Figure S14a** Job's plot for stoichiometry determination of  $[\text{M1}-\text{Y}^{3+}]$  adduct ( $\lambda_{\text{ex}} = 410 \text{ nm}$   $\lambda_{\text{em}} = 527 \text{ nm}$ )

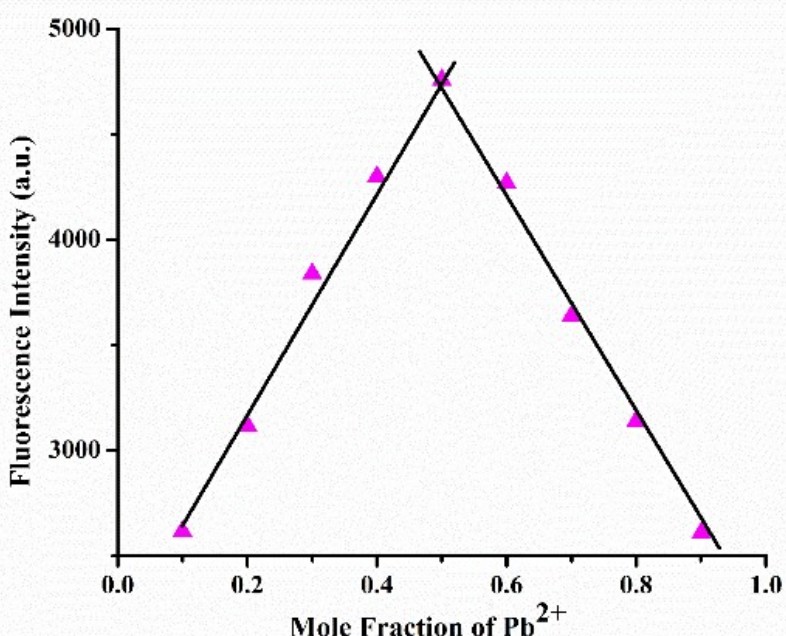


**Figure S14b** Job's plot for stoichiometry determination of  $[\text{M1}-\text{Pb}^{2+}]$  adduct ( $\lambda_{\text{ex}} = 410 \text{ nm}$   $\lambda_{\text{em}} = 463 \text{ nm}$ )

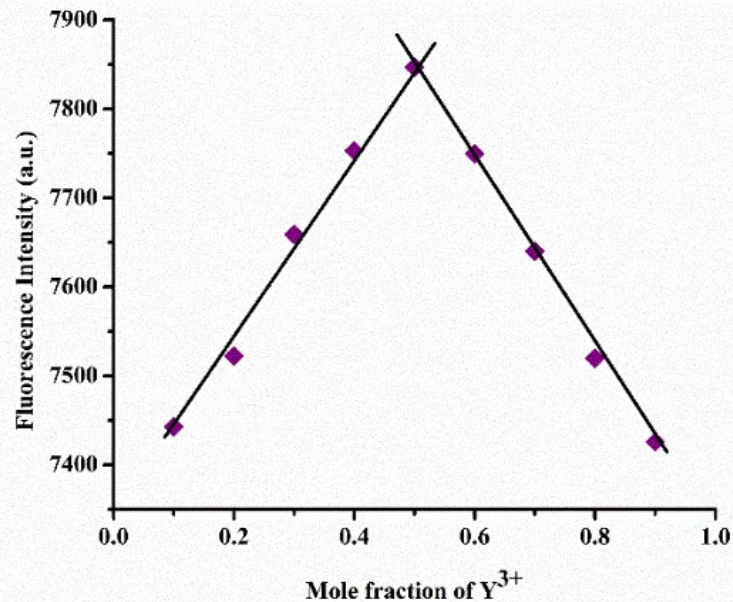


**Figure S14c** Job's plot for stoichiometry determination of  $[\text{M2}-\text{Y}^{3+}]$  adduct ( $\lambda_{\text{ex}} = 342 \text{ nm}$   $\lambda_{\text{em}} = 497 \text{ nm}$ )

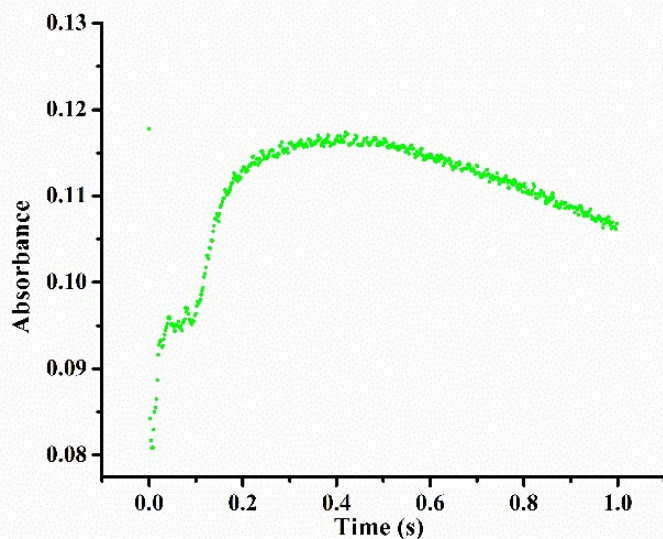


**Figure S15a** Change of absorbance ( $\lambda = 426 \text{ nm}$ ) of  $\text{M1}$  ( $20 \mu\text{M}$ , pH 7.4) saturated with  $\text{Pb}^{2+}$  upon irradiation with 2 MeV electrons (noisy curve)

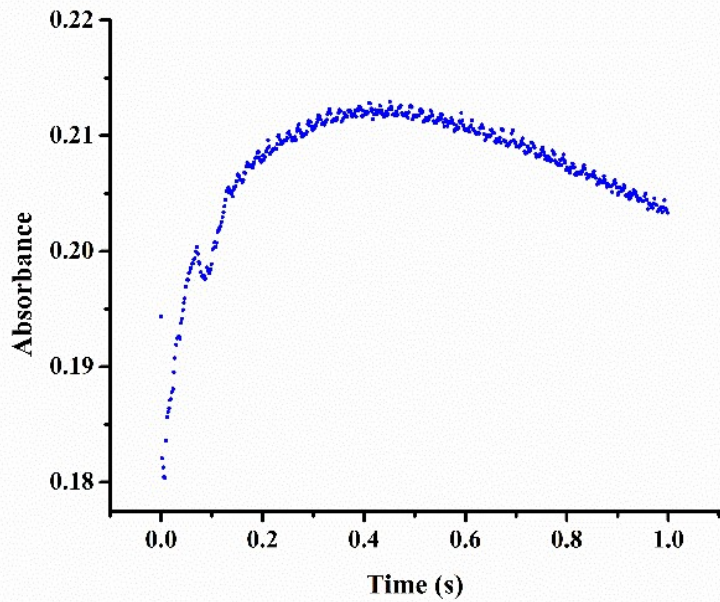


**Figure S15b** Change of absorbance ( $\lambda = 426$  nm) of **M1** (20  $\mu\text{M}$ , pH 7.4) saturated with  $\text{Y}^{3+}$  upon irradiation with 2 MeV electrons (noisy curve)

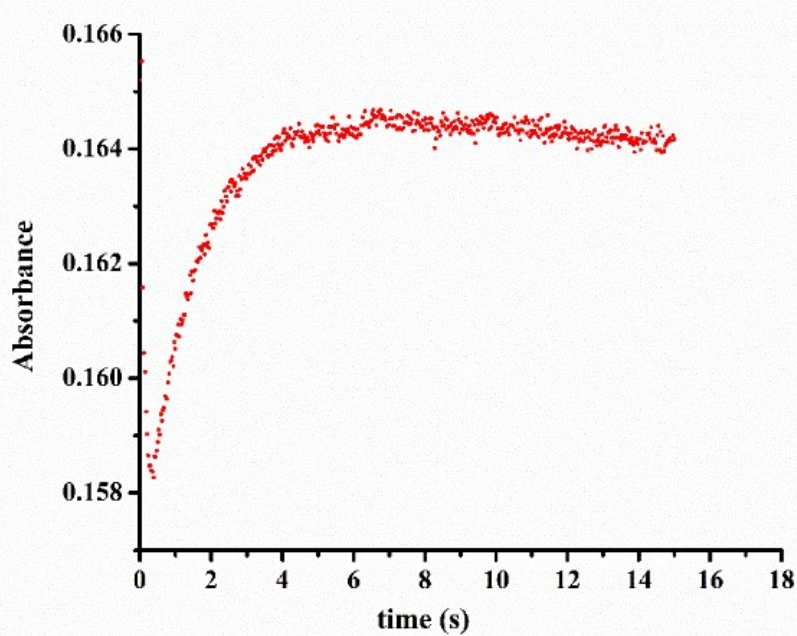


**Figure S15c** Change of absorbance of 20  $\mu\text{M}$  **MM2** at 440 nm (pH 7.4) saturated with  $\text{Y}^{3+}$  upon irradiation with 2 MeV electrons (noisy curve)

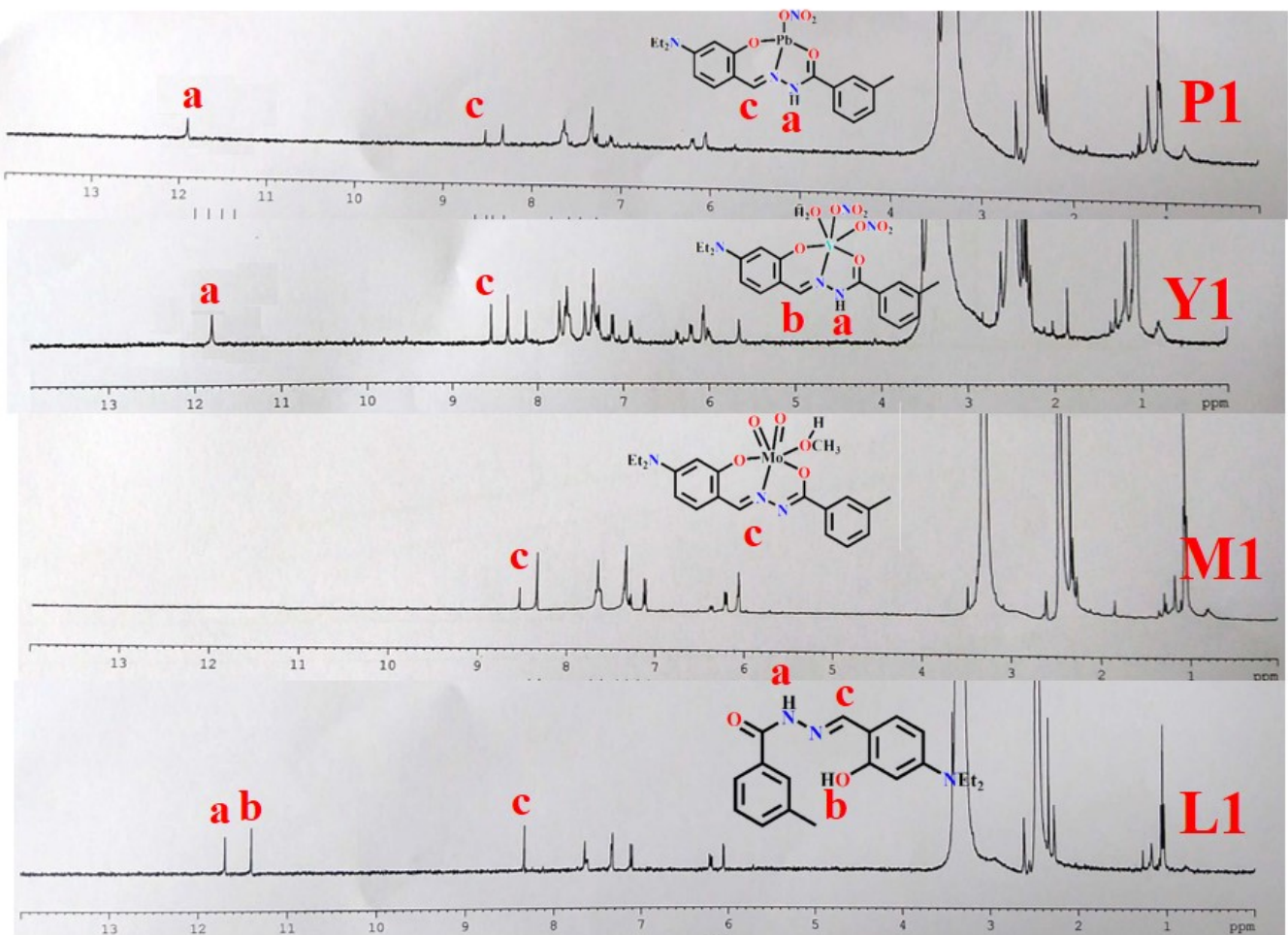


**Figure S16a**  $^1\text{H}$ NMR titration of **M1**with  $\text{Y}^{3+}$  and  $\text{Pb}^{2+}$

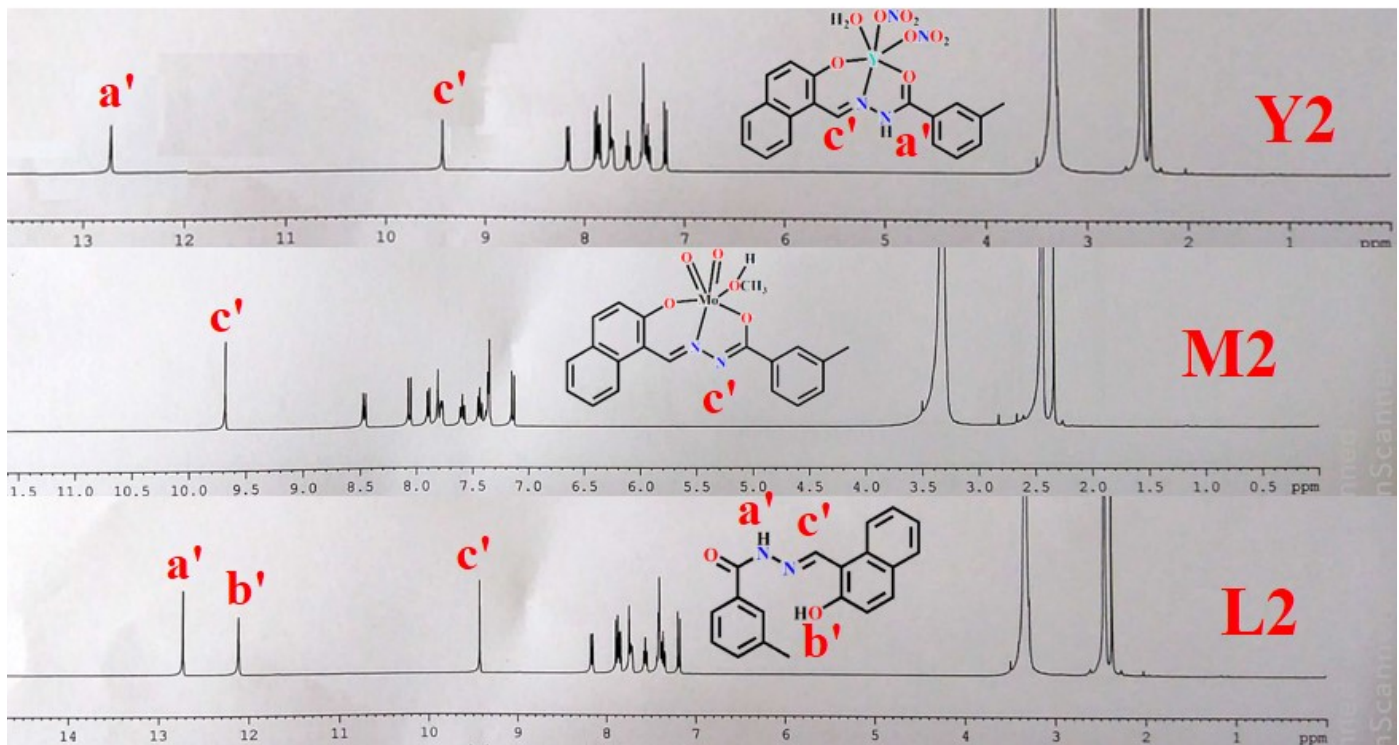


**Figure S16b**  $^1\text{H}$ NMR titration of **M2**with  $\text{Y}^{3+}$

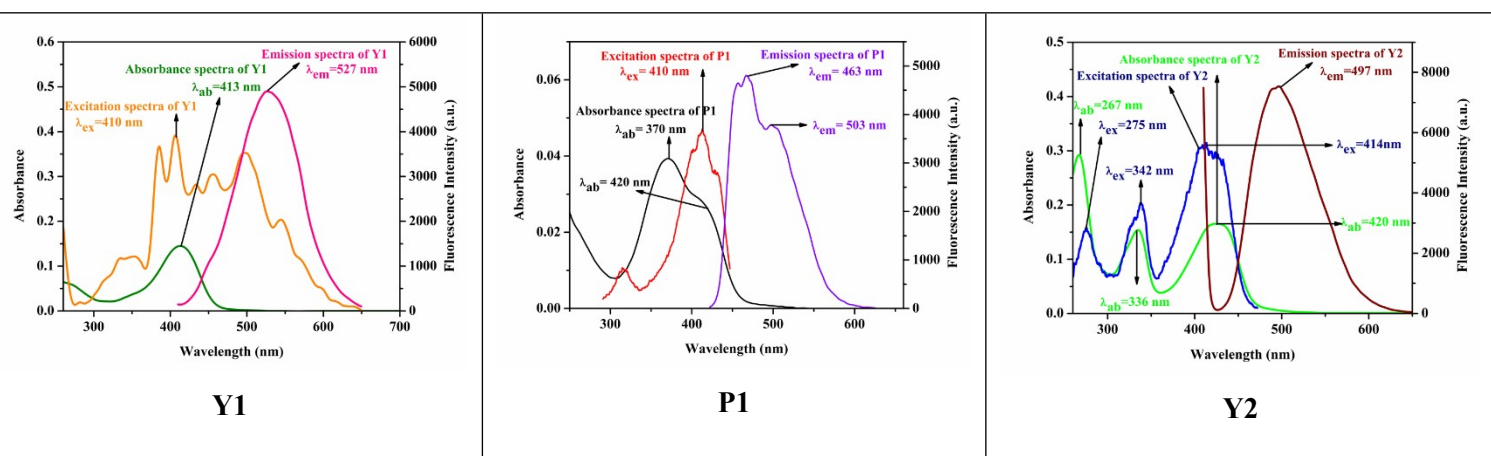


**Figure S17** Excitation, emission and absorption spectra of **Y1**,**P1** and **Y2**; media and pH mentioned *supra*

**Table S1** Comparison among pioneering  $\text{Y}^{3+}$  selective probes

Sl. No.	Media	Method	Mechanism	LOD	Binding constant	Ref.
1.	60% EtOH	Fluorescence method	CHEF	100 ppb	-	61
2.	$\text{H}_2\text{O}$	Colorimetric method	Aggregation	57.7 nM	-	62
3.	THF	Fluorescence method	ICT	13 ppm	$2.70 \times 10^8 \text{ M}^{-1}$	63
4.	-	Fluorescence method	(LIBS-LIF)	0.3 ppm	-	64
5.	Dilute $\text{HNO}_3$	Spectrophotometric method	Precipitation	1 ppm	-	65
6.	EtOH/ $\text{H}_2\text{O}$	Fluorescence method	Metal displacement	$5.5 \times 10^{-7}\text{M}$	$3.9 \times 10^4 \text{ M}^{-1}$	This work

**Table S2** Comparison among pioneering Pb<sup>2+</sup> selective probes

Sl. No.	Media	Sensing mode	Mechanism	LOD	Binding constant	Ref.
1.	CH <sub>3</sub> CN/HEPES (9 : 1, v/v)	Turn-Off	PET	0.5 μM	2.043×10 <sup>3</sup> M <sup>-1</sup>	66
2.	CH <sub>3</sub> CN	Turn-On	CHEF	13.2 nM	6.1 × 10 <sup>5</sup> M <sup>-1</sup>	67
3.	1:9 DMSO/H <sub>2</sub> O (v/v)	Turn-Off	Receptor- metal complex	1.9 nM	6.76 × 10 <sup>6</sup> M <sup>-1</sup>	68
4.	CH <sub>3</sub> CN/H <sub>2</sub> O (2:8)	Turn-On	CHEF	2ppb	-	69
5.	THF/H <sub>2</sub> O	Turn-On	SPR	0.5 μM	-	70
6.	EtOH/H <sub>2</sub> O	Turn-On	Metal displacement	26 nM	2.9×10 <sup>4</sup> M <sup>-1</sup>	Present work

**Table S3** Crystal data and structure refinement for **M1** and **M2**

Crystal parameters	M1	M2
CCDC	<b>1941205</b>	<b>1919499</b>
Empirical formula	C <sub>20</sub> H <sub>24</sub> MoN <sub>3</sub> O <sub>5</sub>	C <sub>20</sub> H <sub>17</sub> MoN <sub>2</sub> O <sub>5</sub>
Formula weight	482.36	461.30
Crystal system	Orthorhombic	Monoclinic
Space group	P n a 21	P 21/c
Hall group	P 2c -2n	-P 2ybc
Temparature	150 K	150 K
Wavelength	0.71073	0.71073
a/Å	13.7533(17)	7.7042(4)
b/Å	20.0569(10)	16.2189(8)
c/Å	7.505(2)	14.9336(7)
α/°	90	90
β/°	90	102.051(2)
γ/°	90	90
Volume/Å <sup>3</sup>	2070.2(6)	1824.89(16)
Z	4	4
ρ <sub>calc</sub> g/cm <sup>3</sup>	1.548	1.679
μ/mm <sup>-1</sup>	0.670	0.755
F(000)	988.0	932.0
F(000')	981.50	925.50
Θmax	25.370	29.180

Index ranges (h,k,lmax)	16,24,9	10,22,20
Reflections collected (R)	0.0843( 2267)	0.0264( 4175)
wR <sub>2</sub> (Reflection)	0.2984( 2976)	0.0703( 4945)
S	1.280	1.074
Npar	266	255
Data completeness	1.45/0.79	0.999

**Table S4a** Selected bond lengths and angles of **M1**

Atoms	Bond length	Atoms	Bond angle
Mo O4	1.69(2)	O4 Mo O5	105.7(10)
Mo O5	1.727(16)	O4 Mo O2	98.2(8)
Mo O2	1.925(15)	O5 Mo O2	103.9(7)
Mo O1	2.012(13)	O4 Mo O1	97.2(9)
Mo N2	2.20(2)	O2 Mo O1	149.8(6)
Mo O3	2.385(17)	O4 Mo N2	94.1(9)
O1 C1	1.29(3)	O5 Mo N2	158.2(9)
O2 C11	1.34(3)	O2 Mo N2	81.9(7)
O3 C20	1.40(3)	O1 Mo N2	71.1(7)
N1 C1	1.28(3)	O4 Mo O3	170.3(8)
N1 N2	1.43(3)	O5 Mo O3	83.9(8)
N2 C9	1.34(3)	O2 Mo O3	80.7(6)
N3 C13	1.38(3)	O1 Mo O3	79.8(8)
N3 C18	1.49(4)	N2 Mo O3	76.2(7)
N3 C16	1.53(3)	C1 O1 Mo	119.1(14)
C1 C2	1.51(3)	C11 O2 Mo	133.1(16)
C2 C3	1.40(3)	C20 O3 Mo	128.8(14)
C2 C7	1.42(3)	C1 N1 N2	105.5(18)
C3 C4	1.38(3)	C9 N2 N1	116(2)
C4 C5	1.37(3)	C9 N2 Mo	126.2(17)
C4 C8	1.56(3)	N1 N2 Mo	117.0(12)
C5 C6	1.35(3)	C13 N3 C18	123(2)
C6 C7	1.43(3)	C13 N3 C16	122(2)
C9 C10	1.38(3)	C18 N3 C16	113(2)
C10 C11	1.45(3)	N1 C1 O1	127(2)
C10 C15	1.46(3)	N1 C1 C2	118(2)
C11 C12	1.43(3)	O1 C1 C2	115.5(19)
C12 C13	1.39(3)	C3 C2 C7	118(2)
C13 C14	1.37(4)	C3 C2 C1	119(2)
C14 C15	1.33(3)	C7 C2 C1	124(2)
C16 C17	1.50(4)	C4 C3 C2	122(2)

C18 C19	1.53(4)	C5 C4 C3	118(2)
		C5 C4 C8	120(2)
		C3 C4 C8	122(2)
		C6 C5 C4	124(2)
		C5 C6 C7	119(2)
		C2 C7 C6	119(2)
		N2 C9 C10	126(2)
		C9 C10 C11	123(2)
		C9 C10 C15	123(2)
		C11 C10 C15	114(2)
		O2 C11 C12	119(2)
		O2 C11 C10	120(2)
		C12 C11 C10	121(2)
		C13 C12 C11	118(2)
		C14 C13 N3	120(2)
		C14 C13 C12	123(3)
		N3 C13 C12	117(2)
		C15 C14 C13	121(3)
		C14 C15 C10	123(2)
		C17 C16 N3	109(2)
		N3 C18 C19	111(3)

**Table S4b** Selected bond lengths and angles of M2

Atoms	Bond length	Atoms	Bond angle
Mo O1	2.0093(14)	O2 Mo O1	149.77(6)
Mo O2	1.9286(14)	O3 Mo O1	96.89(6)
Mo O3	1.7046(15)	O3 Mo O2	103.41(7)
Mo O4	1.6945(15)	O4 Mo O1	96.35(7)
Mo O5	2.3456(14)	O4 Mo O2	99.26(7)
Mo N2	2.2269(16)	O4 Mo O3	105.99(8)
O1 C1	1.310(2)	O5 Mo O1	78.51(6)
O2 C11	1.342(2)	O5 Mo O2	82.45(6)
O5 C20	1.401(3)	O5 Mo O3	81.78(6)
N1 N2	1.401(2)	O5 Mo O4	171.28(6)
N1 C1	1.311(2)	N2 Mo O1	72.13(6)
N2 C9	1.294(2)	N2 Mo O2	80.32(6)
C1 C2	1.472(3)	N2 Mo O3	155.41(7)
C2 C3	1.396(3)	N2 Mo O4	97.21(7)
C2 C7	1.393(3)	N2 Mo O5	74.57(5)
C3 C4	1.384(3)	C1 O1 Mo	120.22(12)
C4 C5	1.384(3)	C11 O2 Mo	136.27(13)
C5 C6	1.391(3)	C20 O5 Mo	124.88(15)
C6 C7	1.391(3)	C1 N1 N2	109.62(15)

C6 C8	1.503(3)	N1 N2 Mo	115.19(11)
C9 C10	1.444(2)	C9 N2 Mo	128.85(13)
C10 C11	1.395(3)	C9 N2 N1	115.96(15)
C10 C19	1.449(3)	N1 C1 O1	122.70(17)
C11 C12	1.415(3)	C2 C1 O1	117.50(16)
C12 C13	1.363(3)	C2 C1 N1	119.78(17)
C13 C14	1.416(3)	C3 C2 C1	120.03(18)
C14 C15	1.417(3)	C7 C2 C1	120.44(17)
C14 C19	1.422(3)	C7 C2 C3	119.54(18)
C15 C16	1.367(3)	C4 C3 C2	119.2(2)
C16 C17	1.402(3)	C5 C4 C3	120.7(2)
C17 C18	1.376(3)	C6 C5 C4	121.15(19)
C18 C19	1.412(3)	C7 C6 C5	117.9(2)
		C8 C6 C5	121.3(2)
		C8 C6 C7	120.8(2)
		C6 C7 C2	121.55(19)
		C10 C9 N2	124.51(17)
		C11 C10 C9	121.12(17)
		C19 C10 C9	119.45(17)
		C19 C10 C11	119.30(17)
		C10 C11 O2	123.24(17)
		C12 C11 O2	115.77(17)
		C12 C11 C10	120.93(18)
		C13 C12 C11	120.07(18)
		C14 C13 C12	121.50(18)
		C15 C14 C13	120.68(18)
		C19 C14 C13	119.64(18)
		C19 C14 C15	119.68(19)
		C16 C15 C14	121.13(19)
		C17 C16 C15	119.2(2)
		C18 C17 C16	121.2(2)
		C19 C18 C17	120.99(19)
		C14 C19 C10	118.54(17)
		C18 C19 C10	123.67(17)
		C18 C19 C14	117.79(18)